

Compressed Subspace Learning Based on Canonical Angle Preserving Property

Yuchen Jiao, Gen Li, and Yuantao Gu*

Manuscript submitted July 14, 2019.

Abstract

A standard way to tackle the challenging task of learning from high-dimensional data is to exploit its underlying low-dimensional structure. Union of Subspaces (UoS) is a popular and powerful model to describe such structure which assumes that the data lies in the union of a collection of low-dimensional subspaces. Extracting useful information from UoS structure of data has become the task of the newly-emerged field of subspace learning. In this paper, we investigate how random projection, an efficient and commonly-used method for dimensionality reduction, distorts the UoS structure of data. Here the fine details of UoS structure are described in terms of canonical angles (also known as principal angles) between subspaces, which is a well-known characterization for relative subspace positions by a sequence of angles. It is proved that random projection with the so-called Johnson-Lindenstrauss (JL) property approximately preserves canonical angles between subspaces. As canonical angles completely determine the relative position of subspaces, our result indicates that random projection approximately preserves structure of a union of subspaces. Inspired by this result, we propose in this paper the framework of Compressed Subspace Learning (CSL), which enables to extract useful information from the UoS structure of data in a greatly reduced dimension and has the advantage of lower computational cost and memory requirements. We demonstrate the effectiveness of CSL in various subspace-related tasks such as subspace visualization, active subspace detection, and subspace clustering.

Keywords: Canonical angles, random projection, Johnson-Lindenstrauss property, Union of Subspaces

1 Introduction

Many data analysis tasks in machine learning and data mining deal with real-world data that are presented in high-dimensional spaces, which often brings prohibitively high compu-

*The authors are with Department of Electronic Engineering, Tsinghua University, Beijing 100084, China. The corresponding author of this paper is Y. Gu (gyt@tsinghua.edu.cn).

tational complexity. Attempting to resolve this problem led data scientists to the discovery that many high-dimensional real-world datasets possess some low-dimensional structure that makes them easier to handle. Various models have been proposed to describe such structures, among which the Union of Subspaces (UoS) model is a popular one. It assumes that in a dataset with high ambient dimension, the data points actually lie on a few low-dimensional linear subspaces. This model has successfully characterized the intrinsic low-dimensional structure of many datasets, including face images from multiple individuals, marker trajectories from multiple rigid objectives, hyperspectral images, and gene expression data (Elhamifar and Vidal, 2013, 2009; Zhai et al., 2017; McWilliams and Montana, 2014).

The task of subspace learning is then to extract useful information from UoS structure of data. For example, subspace clustering seeks to find some law of the data distribution, active subspace detection identifies the category of a newly-encountered data point, subspace visualization discovers the correlation and irregularity in the data set. Many algorithms of the above subspace learning tasks have been proposed. The performance of these algorithms has been found closely related to the concept of *subspace structure*¹ (Wang and Yu, 2016; Heckel et al., 2015; Meng et al., 2018; Lodhi and Bajwa, 2018).

There is, however, a natural question that gets unnoticed in the design of these classical algorithms, to cite Donoho (2006), “why go to so much effort to acquire all the data when most of what we get will be thrown away?” In our case, this translates to the following: since UoS structure involves only a collection of low-dimensional subspaces that cost much less to describe than the original high-dimensional representation of all data points, why do we go to so much effort to processing the redundant high-dimensional representation? This motivates us to propose in this paper the framework of Compressed Subspace Learning (CSL), which significantly reduces the sampling and processing complexity of subspace learning by utilizing random projection to map the original data to a space with dimension $O(d)$, where d is the maximal dimension of underlying subspaces in UoS model.

To analytically characterize the impact exerted by random projection on UoS structure, we restrict our attention to a class of random projections with so-called Johnson-Lindenstrauss (JL) property (Foucart and Rauhut, 2013). This choice is advantageous in that JL property is a strong concentration property yet satisfied by a very wide range of random matrices, such as Gaussian matrices, Bernoulli matrices, other sub-Gaussian matrices, and some matrices with fascinating fast algorithms. For such random projection we prove that the UoS structure, described in terms of canonical angles, is approximately preserved after being projected onto a space of dimension $O(d)$. We call this property *Canonical*

¹Here *subspace structure* is a rough concept describing relative subspace positions. It may represent affinity, subspace distances, and canonical angles between subspaces.

Angles Preserving (CAP) property. CAP property forms the theoretical foundation of our CSL framework. We test the power of our framework on several subspace-related tasks, including subspace visualization, active subspace detection, and subspace clustering.

1.1 Random Projection and Its Structure Preserving Property

Among numerous dimensionality reduction methods, linear methods are widely used in practice for their simple geometric interpretations and computational efficiency. The most famous one in this category may be Principal Component Analysis (PCA), which projects the original data onto a low-dimensional space such that the dimensionality-reduced training data has the maximized variance. Random projection is another famous family of linear methods, which reduces the dimension of original data by multiplying it with a fat random matrix. Random projection has the advantage of high computational efficiency and being data-free.

More technically speaking, random projection uses a randomly generated matrix to map the original high-dimensional data in \mathbb{R}^N to a low-dimensional space \mathbb{R}^n , $n < N$. It is, of course, impossible to undertake a comprehensive study on all types of random projections, and practice indicates there are only a few random matrices that are interesting enough to be used for random projection. Typical examples include Gaussian matrices, Bernoulli matrices, other sub-Gaussian matrices, partial Fourier matrices, and partial Hadamard matrices. Though many previous works on random projection and random matrix theory focus on sub-Gaussian matrices, structured random matrices like partial Fourier matrices and partial Hadamard matrices are also important due to computational convenience. In fact, the computational complexity of random projection is $O(Nn)$ for sub-Gaussian matrices, and $O(N \log N)$ for partial Fourier matrices and partial Hadamard matrices. Note that the $O(Nn)$ complexity is at the same level with PCA, while the $O(N \log N)$ complexity is close to optimal since computing the dimensionality-reduced image of a generic N -dimensional vector requires at least $O(N)$ time (to read the input).

It turns out that there is a systematic scheme to treat most of the aforementioned random matrices, most notably the ones with fast algorithms, via JL property (Foucart and Rauhut, 2013; Xu et al., 2019). We will study under this scheme the distortion of subspace structure brought by random projection.

The investigation of distortion on subspace structure induced by random projection fits into the long history of researches on structure preserving property of random projection. Figure 1 depicts some results in this vein. The story begins with the classical Johnson-Lindenstrauss Lemma, which considers the structure of point sets in Euclidean space described by pairwise distance. JL Lemma states that for any a set S consisting of

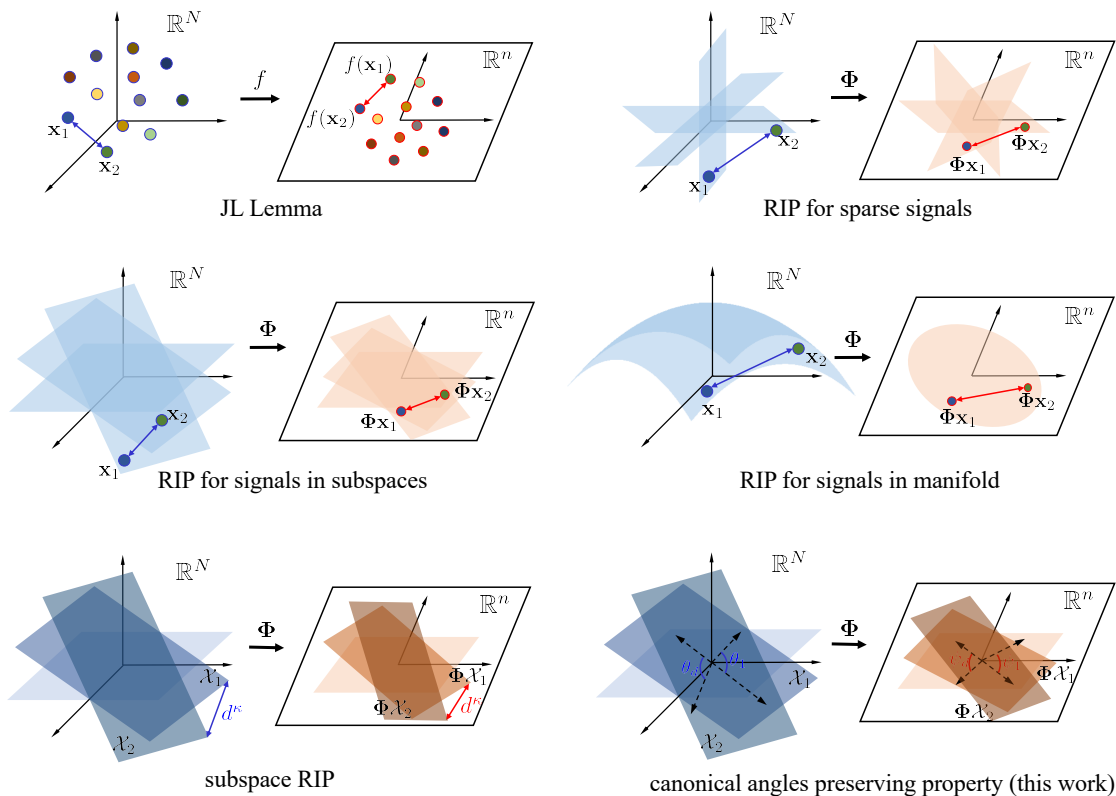


Figure 1: JL Lemma, RIP for sparse signals, RIP for signals in subspaces, RIP for signals in manifold, subspace RIP, and canonical angles preserving property. Notation f , Φ denotes the linear map and random projection from \mathbb{R}^N to \mathbb{R}^n , respectively, $n < N$. Notation \mathbf{x}_i and \mathcal{X}_i denotes the point and d -dimensional subspace in Euclidean space, respectively. Notation d^k denotes the projection Frobenius-norm distance, and θ_k , ψ_k denotes the k -th canonical angle before and after embedding, respectively, $k = 1, \dots, d$.

L points in Euclidean space \mathbb{R}^N , there is a map $f : \mathbb{R}^N \rightarrow \mathbb{R}^n$ where $n = O(\varepsilon^{-2} \log L)$, such that all pairwise Euclidean distances in S are preserved up to a factor of $(1 \pm \varepsilon)$. This result is originally proved by choosing f to be Gaussian random projection (Johnson and Lindenstrauss, 1984). JL Lemma has now become a fundamental lemma in the theory of machine learning. Another notion related to JL Lemma is the classical Restricted Isometry Property (RIP) for sparse signals, which states that all sparse vectors in \mathbb{R}^N with sparsity no more than k can be embedded into $O(k \ln(N/k))$ dimensions with the pairwise Euclidean distances preserved up to $(1 \pm \varepsilon_{2k})$ (Candès, 2008; Baraniuk et al., 2015). It has been proved that sub-Gaussian random matrices and some sparse random matrices satisfy RIP for sparse signals with probability $1 - e^{-O(n)}$ (Eftekhari et al., 2015). This conclusion has remarkably fascinated the researches in Compressed Sensing. More researches show that sub-Gaussian random matrices are able to preserve some other low-dimensional structures, for instance,

pairwise distance of data points on subspaces and manifolds (Dirksen, 2016).

In the recent decade, the powerful UoS model leads to a new point of view that the structure of many real-world datasets is in fact the structure of a collection of subspaces where the data points reside (Eldar and Mishali, 2009; Zhu et al., 2014). In spite of the extensive study in the literature on the distance preserving property for data points, it was not clear whether random projection preserves the distance or more refined structure of subspaces until the emergence of Li and Gu (2018) and Li et al. (2018). In these two papers it is proved that Gaussian random projection can approximately preserve the affinity between two subspaces. These two papers also proved that the so-called projection Frobenius-norm distance of subspaces are approximately preserved and named this property *subspace RIP*. More precisely, in Li et al. (2018) it is stated that any L given subspaces with dimensions at most d can be embedded by Gaussian random matrices into $O(\max\{d, \ln L, \ln(1/\delta)\})$ dimensions with probability $1 - \delta$, such that their pairwise projection Frobenius-norm distances are preserved up to a factor of $(1 \pm \varepsilon)$.

Subspace structure plays an essential role in many algorithms based on UoS model. For example, it has been proved that subspace affinity influences the performance of subspace clustering algorithms, including Sparse Subspace Clustering (SSC) in Elhamifar and Vidal (2013), thresholding-based subspace clustering (TSC) in Heckel and Bölcskei (2015), and SSC via Orthogonal Matching Pursuit (SSC-OMP) in You et al. (2016). When applying these algorithms on dimensionality-reduced datasets, subspace structure preserving property turns out to be a useful tool in analyzing their performance (Meng et al., 2018).

1.2 Canonical Angles

It is well-known that subspace structure is perfectly described by canonical angles, also known as principal angles (Jordan, 1875; Wong, 1967). These are a sequence of acute angles that provide a complete characterization of the relative subspace positions in the following sense:

Theorem 1. (Wong, 1967) If the canonical angles between subspaces $\mathcal{S}_1, \mathcal{S}_2$ are identical with the canonical angles between subspaces $\mathcal{S}'_1, \mathcal{S}'_2$, then there exists an orthogonal transform \mathbf{T} such that $\mathbf{T}\mathcal{S}_1 = \mathcal{S}'_1$, $\mathbf{T}\mathcal{S}_2 = \mathcal{S}'_2$.

It is thus obvious that any other quantity describing relative subspace positions is a function of canonical angles, for example, the affinity between two subspaces (Soltanolkotabi and Candes, 2012), any notion of rotation-invariant subspace distance, including the aforementioned projection Frobenius-norm distance and the widely-used geodesic distance (Ye and Lim, 2016), other definitions of subspace angles, including product angle (Miao and Ben-Israel, 1992, 1996), Friedrichs angle, and Dixmier angle (Deutsch, 1995). See Appendix A

for a discussion on different definitions of subspace distance, and the advantage of canonical angles over these subspace distances in characterizing relative subspace positions.

1.3 Contributions

This work first studies the distortion of canonical angles between subspaces induced by random projection with JL property. We prove that for any L given subspaces with dimensions at most d , they can be mapped to a low-dimensional space \mathbb{R}^n with each canonical angle preserved up to $(1 \pm \varepsilon)$. The requirement on dimension n is given by $n = O(\varepsilon^{-2} \max\{d, \ln L\})$. This result indicates that each canonical angle is approximately preserved by random projection with JL property, and thus is called canonical angle preserving (CAP) property. As canonical angles best characterize the relative subspace positions, CAP property implies that subspace structure also remains almost unchanged. The invariance of other concepts on subspace structure, including various notions of subspace distance, are easily established based on CAP property, which is called subspace RIP in general.

Based on CAP property, we propose a Compressed Subspace Learning (CSL) framework, which aims to reduce the time and storage cost of UoS-based algorithms by taking advantage of the computational efficiency and subspace structure preserving property of random projection. This framework is capable of processing data in a space with almost the lowest possible dimension, i.e., in the same order of the maximal dimension of subspaces.

We demonstrate the power of the aforementioned framework by taking three subspace-learning tasks, namely subspace visualization, active subspace detection, and subspace clustering, as examples. We empirically show that applying CSL can successfully circumvent the curse of dimensionality, and theoretically analyze their performance using CAP property. Considering that CAP property is independent of algorithms, we infer that CSL is a universally effective framework for subspace-related tasks.

1.4 Organization and Notations

The rest of this paper is organized as follows. In Section 2, definitions and basic properties about canonical angles and JL property are provided. In Section 3, we precisely state our main theoretical result, i.e., CAP property, and use it to establish general subspace RIP. Besides, we compare these two results with some well-known or similar works. Based on these theoretical results, we formulate and describe the CSL framework in Section 4. Section 5 is devoted to a full proof of CAP property. In Section 6, we empirically show the effectiveness of CSL framework on three subspace-related tasks. The corresponding performance analysis are deferred to appendix. Finally, in Section 7 we conclude the paper.

Throughout this paper, bold upper and lower case letters are used to denote matrices

and vectors, respectively. Notation \mathbf{V}^T denotes the transposition of matrix \mathbf{V} . Notation $\|\mathbf{v}\|$ denotes the ℓ_2 -norm of vector \mathbf{v} . $\sigma_k(\mathbf{V})$ denotes the k -th singular value of matrix \mathbf{V} in descending order. Letters in calligraphy denote subspaces, such as \mathcal{X} , \mathcal{Y} and \mathcal{S} . The orthogonal complement of subspace \mathcal{S} is denoted by \mathcal{S}^\perp . The projection of vector \mathbf{v} onto subspace \mathcal{S} is denoted as $\mathbf{P}_{\mathcal{S}}(\mathbf{v})$. The $(k-1)$ -dimensional unit sphere is denoted by \mathcal{S}^{k-1} .

2 Preliminary

We now give the precise definition of canonical angles discussed in Section 1.2 as below.

Definition 1. (Galántai and Hegedűs, 2006) Assume there are two subspaces $\mathcal{X}_1, \mathcal{X}_2$ with dimensions $d_1 \leq d_2$. There are d_1 canonical angles $\theta_1, \dots, \theta_{d_1}$ between them, which are recursively defined as

$$\cos \theta_k = \max_{\mathbf{x}_1 \in \mathcal{X}_1} \max_{\mathbf{x}_2 \in \mathcal{X}_2} \frac{\mathbf{x}_1^T \mathbf{x}_2}{\|\mathbf{x}_1\| \|\mathbf{x}_2\|} =: \frac{\mathbf{x}_{1,k}^T \mathbf{x}_{2,k}}{\|\mathbf{x}_{1,k}\| \|\mathbf{x}_{2,k}\|}, \quad k = 1, \dots, d_1,$$

where the maximization is with the constraints $\mathbf{x}_l^T \mathbf{x}_{li} = 0$, $i = 1, \dots, k-1$, $l = 1, 2$. The vectors $(\mathbf{x}_{1,k}, \mathbf{x}_{2,k})$ are the corresponding pairs of principal vectors, $k = 1, \dots, d_1$.

Clearly $0 \leq \theta_1 \leq \dots \leq \theta_{d_1} \leq \pi/2$. We remark that canonical angles are uniquely defined, while principal vectors are not.

An alternative definition of canonical angles and principal vectors via singular values is stated as below, which is equivalent to Definition 1.

Lemma 1. (Björck and Golub, 1973) Let $\mathbf{X}_l \in \mathbb{R}^{m \times d_l}$ be an orthonormal basis for the subspace \mathcal{X}_l with dimension d_l , $l = 1, 2$ and suppose $d_1 \leq d_2$. If we apply singular decomposition on $\mathbf{X}_1^T \mathbf{X}_2$ and get the thin SVD $\mathbf{X}_1^T \mathbf{X}_2 = \mathbf{Q}_1 \mathbf{\Sigma} \mathbf{Q}_2^T$, where $\mathbf{\Sigma} = \text{diag}(\sigma_1, \dots, \sigma_{d_1})$ with $\sigma_1 \geq \dots \geq \sigma_{d_1}$. Then the cosine of the k -th canonical angle θ_k between $\mathcal{X}_1, \mathcal{X}_2$ is defined as

$$\cos \theta_k = \sigma_k, \quad \forall 1 \leq k \leq d_1.$$

Columns of $\mathbf{X}_1 \mathbf{Q}_1$ and $\mathbf{X}_2 \mathbf{Q}_2$ are principal vectors.

It follows from Lemma 1 that

$$\cos \theta_1 = \max_{\substack{\mathbf{x}_1 \in \mathcal{X}_1 \\ \|\mathbf{x}_1\|=1}} \|\mathbf{P}_{\mathcal{X}_2}(\mathbf{x}_1)\|, \quad (1)$$

$$\cos \theta_{d_1} = \min_{\substack{\mathbf{x}_1 \in \mathcal{X}_1 \\ \|\mathbf{x}_1\|=1}} \|\mathbf{P}_{\mathcal{X}_2}(\mathbf{x}_1)\|. \quad (2)$$

In various notions of subspace distance, a natural and fundamental requirement is that the subspace distance $D(\cdot, \cdot)$ should be rotation invariant, i.e., for any orthogonal matrix

$U \in \mathbb{R}^m$, we have $D(U\mathcal{X}_1, U\mathcal{X}_2) = D(\mathcal{X}_1, \mathcal{X}_2)$. In contrast with canonical angles, only using subspace distance is not sufficient to completely characterize the relative subspace positions. More explanation can be found in Appendix A.

Another key concept in the statement of our main result is JL property, which is defined as below.

Definition 2. (Foucart and Rauhut, 2013) A random matrix $\Phi \in \mathbb{R}^{n \times N}$ is said to satisfy Johnson-Lindenstrauss property, if there exists some constant $c > 0$, such that for any $\varepsilon \in (0, 1/2)$ and for any $\mathbf{x} \in \mathbb{R}^N$,

$$P\left(\left|\|\Phi\mathbf{x}\|^2 - \|\mathbf{x}\|^2\right| > \varepsilon \|\mathbf{x}\|^2\right) \leq 2e^{-c\varepsilon^2 n}.$$

JL property is a mild condition satisfied by many random matrices, e.g., sub-Gaussian random matrices, partial Fourier matrices, and partial Hadamard matrices. In addition, Xu et al. (2019) asserts that JL property is implied by classical RIP for sparse signals with sufficiently small restricted isometry constant. Random projection with JL property is called *JL random projection* in this paper.

Remark 1. Our analysis is based on the assumption that the dimension of a low-dimensional subspace \mathcal{X}_l remains unchanged after random projection. For any random matrix with JL property, this assumption is true with probability at least $1 - e^{-O(n)}$ (Xu et al., 2019). In some special cases, such as for Gaussian random matrices, this assumption holds almost surely. We will use this assumption implicitly in all theorems in this paper.

3 Subspace Structure Preserving Property of JL random projection

In this section, we will address our main problem, i.e., the distortion of subspace structure, or equivalently, canonical angles, induced by JL random projection. Based on this result, we establish a general subspace RIP that works for any notion of subspace distance. In addition, we compare our results with some well-known conclusions including JL Lemma and some other similar works.

3.1 Main Result

Our main result, i.e., canonical angles preserving property of JL random projection, is stated in the following theorem.

Theorem 2. Suppose $\Phi \in \mathbb{R}^{n \times N}$ is a random matrix with Johnson-Lindenstrauss property, $n < N$. Suppose $\mathcal{X}_1, \dots, \mathcal{X}_L \subset \mathbb{R}^N$ are L subspaces with dimensions $d_1, \dots, d_L \leq d$. Denote

by $\mathcal{Y}_l \subset \mathbb{R}^n$ the image of \mathcal{X}_l under Φ , $l = 1, \dots, L$. The k -th canonical angle between $\mathcal{X}_i, \mathcal{X}_j$, and $\mathcal{Y}_i, \mathcal{Y}_j$ is denoted as $\theta_k^{i,j}$ and $\psi_k^{i,j}$, respectively. There exist universal positive constants c_1, c_2 , such that for any $1 \leq i, j \leq L$, any $\varepsilon \in (0, 1/2)$, and any $n > c_1 \varepsilon^{-2} \max\{d, \ln L\}$, with probability at least $1 - e^{-c_2 \varepsilon^2 n}$, we have

$$(1 - \varepsilon) \theta_k^{i,j} \leq \psi_k^{i,j} \leq (1 + \varepsilon) \theta_k^{i,j}, \quad \forall 1 \leq k \leq \min\{d_i, d_j\}. \quad (3)$$

Proof. The proof is postponed to Section 5. \square

According to Theorem 2, when $n = O(\varepsilon^{-2} \max\{d, \ln L\})$, each canonical angle between any two subspaces changes only by a small portion less than ε , with overwhelming probability $1 - e^{-c_2 \varepsilon^2 n}$. Thus we call Theorem 2 *canonical angles preserving* (CAP) property.

As an application of the powerful Theorem 2, we give a very short proof of a more general version of subspace RIP in Xu et al. (2019).

Theorem 3. Under the same setting as Theorem 2, there exist universal positive constants c_1, c_2 , such that for any $1 \leq i, j \leq L$, any $\varepsilon \in (0, 1/2)$, and any $n > c_1 \varepsilon^{-2} \max\{d, \ln L\}$, with probability at least $1 - e^{-c_2 \varepsilon^2 n}$, we have

$$(1 - \varepsilon) D(\mathcal{X}_i, \mathcal{X}_j) \leq D(\mathcal{Y}_i, \mathcal{Y}_j) \leq (1 + \varepsilon) D(\mathcal{X}_i, \mathcal{X}_j), \quad \forall d_i \leq d_j, \quad (4)$$

provided that subspace distance $D(\cdot, \cdot)$ can be written as a Lipschitz continuous function of the canonical angles $\boldsymbol{\theta}^{i,j} := [\theta_1^{i,j}, \dots, \theta_{d_i}^{i,j}]^T$ between these two subspaces, and

$$\liminf_{\boldsymbol{\theta} \rightarrow \mathbf{0}} \frac{f(\boldsymbol{\theta})}{\|\boldsymbol{\theta}\|} > 0. \quad (5)$$

In particular, if f is continuously differentiable, $f'(\mathbf{0}) \geq \mathbf{0}$ and $f'(\mathbf{0}) \neq \mathbf{0}$, i.e., any entry of $f'(\mathbf{0})$ is non-negative and at least one entry is positive, then f satisfies the above conditions.

Proof. Denote the k -th canonical angle between $\mathcal{X}_1, \mathcal{X}_2$ and $\mathcal{Y}_1, \mathcal{Y}_2$, respectively, as θ_k and ψ_k . According to Theorem 2, we have

$$\|\boldsymbol{\psi} - \boldsymbol{\theta}\| \leq \varepsilon \|\boldsymbol{\theta}\|.$$

Noticing that f is Lipschitz continuous, we have

$$\begin{aligned} \frac{|f(\boldsymbol{\psi}) - f(\boldsymbol{\theta})|}{f(\boldsymbol{\theta})} &\leq \|f\|_{\text{Lip}} \frac{\|\boldsymbol{\psi} - \boldsymbol{\theta}\|}{f(\boldsymbol{\theta})} \\ &\leq \|f\|_{\text{Lip}} \frac{\|\boldsymbol{\theta}\|}{f(\boldsymbol{\theta})} \varepsilon, \end{aligned} \quad (6)$$

where $\|f\|_{\text{Lip}}$ denotes the Lipschitz constant of f . It suffices to show that $\frac{\|\boldsymbol{\theta}\|}{f(\boldsymbol{\theta})}$ is bounded, which follows easily from $\liminf_{\boldsymbol{\theta} \rightarrow \mathbf{0}} \frac{f(\boldsymbol{\theta})}{\|\boldsymbol{\theta}\|} > 0$ and the continuity of f . \square

Remark 2. We have discussed the invariant property of some concepts about subspace structure, namely, canonical angles and subspace distances. In the study of subspace clustering, another concept about subspace structure, the so-called affinity, was proposed in Soltanolkotabi and Candes (2012). The best conclusion on the invariance of affinity is recently presented in Xu et al. (2019). This result is also an easy consequence of CAP property.

3.2 Related Works

The statement of Theorem 2 resembles that of Johnson-Lindenstrauss Lemma, which is a fundamental and valuable tool in the study of dimensionality reduction. It states that for any set of finite data points in a high-dimensional Euclidean space, they can be embedded into a low-dimensional space with all pairwise distances almost preserved. The precise form of JL Lemma reads as follows.

Lemma 2. (Johnson and Lindenstrauss, 1984) For any set \mathcal{V} of L points in \mathbb{R}^N , there exists a map $f : \mathbb{R}^N \rightarrow \mathbb{R}^n$, $n < N$, such that for all $\mathbf{x}_1, \mathbf{x}_2 \in \mathcal{V}$,

$$(1 - \varepsilon) \|\mathbf{x}_1 - \mathbf{x}_2\|^2 \leq \|f(\mathbf{x}_1) - f(\mathbf{x}_2)\|^2 \leq (1 + \varepsilon) \|\mathbf{x}_1 - \mathbf{x}_2\|^2,$$

if n is a positive integer satisfying $n \geq 4 \ln L / (\varepsilon^2/2 - \varepsilon^3/3)$, where $\varepsilon \in (0, 1)$ is a constant.

We observe that the embedded dimension n required by Theorem 2 coincides with the requirement in JL Lemma. For the special case $d = 1$ in Theorem 2, subspace reduces to a pair of data points lying on unit sphere, and the required $n = O(\varepsilon^{-2} \ln L)$ coincides with that in JL Lemma.

Another notion related to JL Lemma is RIP for sparse signals, a fundamental tool in the theory of Compressed Sensing. Li and Gu (2018) and Li et al. (2018) extend such concept to the so-called subspace RIP, which characterizes the ability of random projection to preserve the projection Frobenius-norm distance between subspaces. This work studies the preserving property of random projection on canonical angles, which is powerful to describe relative subspace positions than certain subspace distance.

Though similar in form, our conclusion differs in many aspects from JL Lemma and RIP, and is not a trivial extension of them. First, Theorem 2 investigates subspaces in Euclidean space instead of points, which makes it a valuable tool in the analysis of UoS model. In addition, Theorem 2 focuses on canonical angles, which better characterize relative subspace positions than any notion of distance. Furthermore, our proof deviates from that of JL Lemma and RIP for sparse signals, and no existing RIP for point sets are invoked in the proof.

In our very previous work Jiao et al. (2017), the preserving property of canonical angles after Gaussian random projection, which is a special case of this work, has been studied. It states that the cosine of each canonical angle between two embedded subspaces distributes around its concentration with certain probability after Gaussian random projection. When the embedded dimension n is large enough, the probability bound is polynomial in n , which is not as optimal as the exponential order in this work. Our another previous work Jiao et al. (2018b) finds an improved relationship $n = O(\ln(1/\delta))$ between the embedded dimension n and the failing probability δ . Compared with Jiao et al. (2018b), this work provides a conclusion for a wider class of random matrices, including partial Fourier matrices which are much more useful than the Gaussian.

The preserving property of projection Frobenius-norm distance has been studied in Li and Gu (2018), Li et al. (2018), and Xu et al. (2019). Li and Gu (2018) and Li et al. (2018) study this problem in Gaussian case. The requirement on embedded dimension n in Li and Gu (2018) in terms of failing probability is $n = O(1/\delta)$. Li et al. (2018) improves it to $n = O(\ln(1/\delta))$. More similar with this work, Xu et al. (2019) studies subspace distance preserving problem for JL random projection. Compared with Li et al. (2018) and Xu et al. (2019), this work establishes subspace RIP for more subspace distance definitions. The proof deviates from that of Li et al. (2018) and Xu et al. (2019) in that we use canonical angles preserving property as the mathematical engine behind our theory. The previous works deal with affinity as a whole and do not focus on each canonical angle. This is why its proof is specific to projection Frobenius-norm distance, and hard to be borrowed by the analysis of other distance definitions.

There are many other works that are similar to our work in formal. Arriaga and Vempala (1999), Haupt and Nowak (2007), and Shi et al. (2012) prove the angle preserving property for vectors. The last two tackle this problem by the RIP for sparse signals, in that the embedded angle can be determined by the embedded vectors. This technique cannot be used in the proof of this work due to the complicated variational nature of the definition of canonical angles. Eftekhari and Wakin (2017) proves that the largest canonical angle between tangent subspaces on the manifold remains nearly unchanged under a linear near-isometry map, for sufficiently close points on the manifold (Proposition 5). The conclusion in this work has no restriction on subspaces. Besides, we study each canonical angle rather than only the largest one. Frankl and Maehara (1990) and Absil et al. (2006) study the distribution of canonical angles between random subspaces. In both these works, randomness exists in the subspace itself. While in this work, it is in the process of embedding, and thus characterize the ability of this dimensionality reduction method to preserve subspace structure. Finally, we remark that Dirksen (2016) is easily mistaken for subspace RIP. In fact, the target of analysis in Dirksen (2016) is the data points lying on union of subspaces,

Algorithm 1 The Framework for Compressed Subspace Learning (CSL)

Input: Original dataset $\{\mathbf{x}_i\}_{i=1,2,\dots}, \mathbf{x}_i \in \mathbb{R}^N$;
The dimension after compression $n, n < N$;
A selected UoS-based learning algorithm \mathcal{A} .

Output: Information $\{\mathbf{o}_i\}_{i=1,2,\dots}$ extracted from the input dataset.

Step I. Applying random projection with partial Fourier matrices

1. Multiplying each entry of \mathbf{x}_i by a Rademacher random variable and getting the sign-randomized version $\tilde{\mathbf{x}}_i$ of data $\mathbf{x}_i, i = 1, 2, \dots,$
2. Computing the fast fourier transformation $\hat{\mathbf{x}}_i$ of the sign-randomized data $\tilde{\mathbf{x}}_i, i = 1, 2, \dots.$
3. Randomly sampling n rows from $\hat{\mathbf{x}}_i$ and constructing the compressed data $\mathbf{y}_i \in \mathbb{R}^n, i = 1, 2, \dots.$

Step II. Conducting the selected algorithm on the compressed data

$$\{\mathbf{o}_i\}_{i=1,2,\dots} = \mathcal{A}(\{\mathbf{y}_i\}_{i=1,2,\dots}).$$

but not subspace itself.

4 Compressed Subspace Learning: A Framework

4.1 Description of CSL Framework

With the CAP property of random projection established, we are now in the position to formulate the aforementioned Compressed Subspace Learning framework, which is done in Algorithm 1. Note that the use of partial Fourier matrices there is not essential and can be replaced by any random matrices with fast algorithms and JL property. According to Theorem 2, in Step I the dimension of data can be compressed to $O(d)$ without destructing the UoS structure, thus the framework allows for significantly boosted computations while guaranteeing the performance to be as good as directly applying algorithm \mathcal{A} without compression. Some concrete applications of this framework are presented in Section 6.

4.2 Related Works

In many problems, e.g., ℓ_2 -regression and support vector machine (SVM) problem, the performance of certain type of random projection as a preprocessing step has been studied. For ℓ_2 regression problem $\mathbf{x}^* = \arg \min_{\mathbf{x}} \|\mathbf{b} - \mathbf{A}\mathbf{x}\|$, it is proved that uniform sampling approximately preserves the least square solution \mathbf{x}^* (Drineas et al., 2006). The requirement on the compressed dimension n in terms of approximation error ε and failing probability

δ is $n = O(M^2 \varepsilon^{-2} \ln(1/\delta))$. In the study of SVM, Shi et al. (2012) discovers the almost invariant property of margin after Gaussian random projection, and gives the condition on the compressed dimension n in terms of the margin distortion ε and failing probability δ as $n = O(\varepsilon^{-2} \ln(1/\delta))$, Paul et al. (2013) considers more types of random projections, including some of those with structured random matrices.

Different from previous works, our study is not constrained to specific algorithms. For example, the framework presented in Algorithm 1 is able to subsume three very different algorithms handling different problems presented in Section 6. Such universality is made possible only by the powerful mathematical engine of CAP property. With this powerful engine, it is possible to adopt the CSL framework to handle many other subspace-related problems and give a complete performance analysis.

5 The Proof of Theorem 2

5.1 Reducing to the case $L = 2$

This part is standard. Assume the conclusion of Theorem 2 is true for $L = 2$. For general L , it follows from this special case that (3) holds with probability at least $1 - \frac{L(L-1)}{2} e^{-c_2 \varepsilon^2 n}$, given that $n > c_1 \varepsilon^{-2} d$. Thus for $n > \frac{2}{c_2 \varepsilon^2} \log(L(L-1))$ and $n > c_1 \varepsilon^{-2} d$, inequality (3) holds with probability at least $1 - e^{-c_2 \varepsilon^2 n/2}$. The conclusion follows by adjusting the values of c_1 and c_2 .

5.2 A Two-sided Bound of ψ_k

We begin by giving $\sin^2 \psi_k$ a two-sided bound which is easier to handle.

Lemma 3. Under the same setting as Theorem 2, assume the k -th principal vectors between \mathcal{X}_1 and \mathcal{X}_2 are given by $\mathbf{u}_{1,k} \in \mathcal{X}_1$ and $\mathbf{u}_{2,k} \in \mathcal{X}_2$. Denote $\varphi_{1,k,k}$ as the largest canonical angle between subspace $\mathcal{Y}_{1,1:k} := \text{span}\{\Phi \mathbf{u}_{1,1}, \dots, \Phi \mathbf{u}_{1,k}\}$ and \mathcal{Y}_2 . Denote $\varphi_{k,d_1,1}$ as the smallest canonical angle between subspace $\mathcal{Y}_{1,k:d_1} := \text{span}\{\Phi \mathbf{u}_{1,k}, \dots, \Phi \mathbf{u}_{1,d_1}\}$ and \mathcal{Y}_2 . The k -th embedded canonical angle ψ_k between the embedded subspaces \mathcal{Y}_1 and \mathcal{Y}_2 is bounded by

$$\varphi_{k,d_1,1} \leq \psi_k \leq \varphi_{1,k,k}.$$

According to the definition of canonical angles, dealing with the largest canonical angle $\varphi_{1,k,k}$ or the smallest canonical angle $\varphi_{k,d_1,1}$ is much easier than dealing with the k -th canonical angle ψ_k . The reason is that ψ_k is recursively defined and it relies on k pairs of principal vectors. While $\varphi_{1,k,k}$ and $\varphi_{k,d_1,1}$ only involve solving a maximization or minimization problem by (1) and (2).

The proof of Lemma 3 is an application of von Neumann min-max theorem.

It suffices to prove that

$$\sin^2 \varphi_{k,d_1,1} \leq \sin^2 \psi_k \leq \sin^2 \varphi_{1,k,k}.$$

We first establish the relationship between $\sin \psi_k$ and $\sin \varphi_{1,k,k}$. Denote \mathbf{V}_i as the orthonormal basis of \mathcal{Y}_i , $i = 1, 2$. We calculate $\sin \psi_k$ via von Neumann min-max theorem as below.

$$\begin{aligned} \sin^2 \psi_k &= 1 - \sigma_k^2(\mathbf{V}_2^T \mathbf{V}_1) \\ &= 1 - \max_{\mathcal{S}^{k-1} \subset \mathbb{R}^{d_1}} \min_{\mathbf{x} \in \mathcal{S}^{k-1}} \|\mathbf{V}_2^T \mathbf{V}_1 \mathbf{x}\|^2, \quad \forall 1 \leq k \leq d_1. \end{aligned} \quad (7)$$

Denote the orthonormal basis of the k -dimensional subspace spanned by \mathcal{S}^{k-1} as $\mathbf{Q} \in \mathbb{R}^{d_1 \times k}$. We have $\{\mathbf{V}_1 \mathbf{x} : \mathbf{x} \in \mathcal{S}^{k-1}\} = \{\mathbf{y} : \mathbf{y} \in \mathcal{C}(\mathbf{V}_1 \mathbf{Q}), \|\mathbf{y}\| = 1\}$, where $\mathcal{C}(\mathbf{V}_1 \mathbf{Q})$ denotes the column space of matrix $\mathbf{V}_1 \mathbf{Q}$. Replacing $\mathbf{V}_1 \mathbf{x}$ with \mathbf{y} in (7), we have

$$\sin^2 \psi_k = 1 - \max_{\mathbf{Q} \in \mathbb{R}^{d_1 \times k}} \min_{\substack{\|\mathbf{y}\|=1 \\ \mathbf{y} \in \mathcal{C}(\mathbf{V}_1 \mathbf{Q})}} \|\mathbf{V}_2^T \mathbf{y}\|^2, \quad \forall 1 \leq k \leq d_1.$$

Noticing that $\|\mathbf{V}_2^T \mathbf{y}\|$ is the norm of the projection of \mathbf{y} onto \mathcal{Y}_2 , and the norm of \mathbf{y} equals 1, we can further simplify the above expression as

$$\begin{aligned} \sin^2 \psi_k &= 1 - \max_{\mathbf{Q} \in \mathbb{R}^{d_1 \times k}} \min_{\substack{\|\mathbf{y}\|=1 \\ \mathbf{y} \in \mathcal{C}(\mathbf{V}_1 \mathbf{Q})}} \|\mathbf{P}_{\mathcal{Y}_2}(\mathbf{y})\|^2 \\ &= \min_{\mathbf{Q} \in \mathbb{R}^{d_1 \times k}} \max_{\substack{\|\mathbf{y}\|=1 \\ \mathbf{y} \in \mathcal{C}(\mathbf{V}_1 \mathbf{Q})}} \|\mathbf{P}_{\mathcal{Y}_2^\perp}(\mathbf{y})\|^2. \end{aligned} \quad (8)$$

Now the RHS of (8) is the projection norm of some unit vector. By taking \mathbf{Q} as $\mathbf{Q}_u := [\mathbf{V}_1^T \mathbf{a}_{1,1}, \dots, \mathbf{V}_1^T \mathbf{a}_{1,k}]$, and plugging (1), we have

$$\begin{aligned} \sin^2 \psi_k &\leq \max_{\substack{\|\mathbf{y}\|=1 \\ \mathbf{y} \in \mathcal{C}(\mathbf{V}_1 \mathbf{Q}_u)}} \|\mathbf{P}_{\mathcal{Y}_2^\perp}(\mathbf{y})\|^2 \\ &= \max_{\substack{\|\mathbf{y}\|=1 \\ \mathbf{y} \in \mathcal{Y}_{1,1:k}}} \|\mathbf{P}_{\mathcal{Y}_2^\perp}(\mathbf{y})\|^2 \\ &= \sin^2 \varphi_{1,k,k}. \end{aligned} \quad (9)$$

It is the turn of $\sin \varphi_{k,d_1,1}$. We need to discover its connection with $\sin \psi_k$. To this end,

we derive step by step the counterparts of (7), (8), and (9) as

$$\begin{aligned}
\sin^2 \psi_k &= 1 - \sigma_k^2 (\mathbf{V}_2^T \mathbf{V}_1) \\
&= 1 - \min_{\mathbf{S}^{d_1-k} \subset \mathbb{R}^{d_1}} \max_{\mathbf{x} \in \mathbf{S}^{d_1-k}} \|\mathbf{V}_2^T \mathbf{V}_1 \mathbf{x}\|^2 \\
&= \max_{\mathbf{Q} \in \mathbb{R}^{d_1 \times (d_1-k+1)}} \min_{\substack{\|\mathbf{y}\|=1 \\ \mathbf{y} \in \mathcal{C}(\mathbf{V}_1 \mathbf{Q})}} \left\| \mathbf{P}_{\mathcal{Y}_2^\perp}(\mathbf{y}) \right\|^2 \\
&\geq \min_{\substack{\|\mathbf{y}\|=1 \\ \mathbf{y} \in \mathcal{C}(\mathbf{V}_1 \mathbf{Q}_l)}} \left\| \mathbf{P}_{\mathcal{Y}_2^\perp}(\mathbf{y}) \right\|^2 \\
&= \min_{\substack{\|\mathbf{y}\|=1 \\ \mathbf{y} \in \mathcal{Y}_{1,k;d_1}}} \left\| \mathbf{P}_{\mathcal{Y}_2^\perp}(\mathbf{y}) \right\|^2 \\
&= \sin^2 \varphi_{k,d_1,1}, \quad \forall 1 \leq k \leq d_1,
\end{aligned} \tag{10}$$

where $\mathbf{Q}_l := [\mathbf{V}_1^T \mathbf{a}_{1,k}, \dots, \mathbf{V}_1^T \mathbf{a}_{1,d_1}]$, and equation (10) uses the relationship between the projection norm and the smallest canonical angle shown in (2).

5.3 Proof of the Canonical Angle Sine Preserving Property

In this subsection, we will prove the following lemma based on Lemma 3.

Lemma 4. Under the same setting as Theorem 2, there exist universal positive constants c_1, c_2 , such that for any $1 \leq i, j \leq L$, any $\varepsilon \in (0, 1/2)$, and any $n > c_1 \varepsilon^{-2} \max\{d, \ln L\}$, with probability at least $1 - e^{-c_2 \varepsilon^2 n}$, we have

$$(1 - \varepsilon) \sin \theta_k^{i,j} \leq \sin \psi_k^{i,j} \leq (1 + \varepsilon) \sin \theta_k^{i,j}, \quad \forall 1 \leq k \leq \min\{d_i, d_j\}. \tag{11}$$

Thanks to the proof in Section 5.1, it suffices to consider canonical angles between two subspaces $\mathcal{X}_1, \mathcal{X}_2$. For convenience, we omit the superscript and denote the k -th (resp. embedded) canonical angle as θ_k (resp. ψ_k).

There are d_1 canonical angles with the assumption $d_1 \leq d_2$. We will prove that the k -th canonical angle satisfies (11). With a similar argument in Section 5.1, this would suffice to show that (11) holds simultaneously for all k .

Therefore, we only need to consider the k -th canonical angle, where k is an integer in $[1, d_1]$. According to Lemma 3, we only need to prove

$$P(\sin \varphi_{1,k,k} \leq (1 + \varepsilon) \sin \theta_k) \geq 1 - e^{-c_2 \varepsilon^2 n}, \tag{12}$$

$$P(\sin \varphi_{k,d_1,1} \geq (1 - \varepsilon) \sin \theta_k) \geq 1 - e^{-c_2 \varepsilon^2 n}. \tag{13}$$

We will complete these in the following two parts. We will follow the notations in Lemma 3. Denote $\mathbf{U}_i := [\mathbf{u}_{i,1}, \dots, \mathbf{u}_{i,d_i}]$ as an orthonormal basis for the original subspace \mathcal{X}_i given by principal vectors, where $i = 1, 2$. We further define $\mathbf{A}_i := \Phi \mathbf{U}_i$, as a basis for the embedded subspace \mathcal{Y}_i , where the k -th column $\mathbf{a}_{i,k}$ is obtained by $\mathbf{a}_{i,k} := \Phi \mathbf{u}_{i,k}$, $k = 1, \dots, d_i$, $i = 1, 2$.

5.3.1 Proof of (12)

According to (1) both $\sin \varphi_{1,k,k}$ and $\sin \theta_k$ can be written as the solution of a maximum problem as below.

$$\begin{aligned}\sin^2 \varphi_{1,k,k} &= \max_{\mathbf{x} \in \mathbf{S}^{k-1}} \left\| \mathbf{P}_{\mathcal{Y}_2^\perp} \left(\frac{\mathbf{A}_{1,1:k} \mathbf{x}}{\|\mathbf{A}_{1,1:k} \mathbf{x}\|} \right) \right\|^2, \\ \sin^2 \theta_k &= \max_{\mathbf{x} \in \mathbf{S}^{k-1}} \left\| \mathbf{P}_{\mathcal{X}_2^\perp} (\mathbf{U}_{1,1:k} \mathbf{x}) \right\|^2.\end{aligned}$$

Then

$$\begin{aligned}\sin^2 \varphi_{1,k,k} - \sin^2 \theta_k &= \max_{\mathbf{x} \in \mathbf{S}^{k-1}} \left\| \mathbf{P}_{\mathcal{Y}_2^\perp} \left(\frac{\mathbf{A}_{1,1:k} \mathbf{x}}{\|\mathbf{A}_{1,1:k} \mathbf{x}\|} \right) \right\|^2 - \sin^2 \theta_k \\ &\leq \max_{\mathbf{x} \in \mathbf{S}^{k-1}} \left[\left\| \mathbf{P}_{\mathcal{Y}_2^\perp} \left(\frac{\mathbf{A}_{1,1:k} \mathbf{x}}{\|\mathbf{A}_{1,1:k} \mathbf{x}\|} \right) \right\|^2 - \left\| \mathbf{P}_{\mathcal{X}_2^\perp} (\mathbf{U}_{1,1:k} \mathbf{x}) \right\|^2 \right].\end{aligned}\quad (14)$$

The RHS of (14) involves the maximum over the whole sphere \mathbf{S}^{k-1} , which can be handled by a standard entropy argument (Appendix F). We may take an ε -net of the unit sphere. Then it suffices to consider any given \mathbf{x} , and use union bound to complete proof.

Here we need to invoke the following lemma about the perturbation on orthonormal basis.

Lemma 5. (Xu et al. (2019), Lemma 6) Suppose \mathbf{U} is an $N \times d$ matrix with orthonormal columns, i.e., $\mathbf{U}^\top \mathbf{U} = \mathbf{I}_d$. Let Φ be an $n \times N$ random matrix with JL property. Then there exist universal positive constants c_1, c_2 , such that for any $\varepsilon < (0, 1/2)$, any $n > c_1 \varepsilon^{-2} d$, we have

$$P(1 - \varepsilon < \sigma_d(\Phi \mathbf{U}) \leq \sigma_1(\Phi \mathbf{U}) < 1 + \varepsilon) \geq 1 - e^{-c_2 \varepsilon^2 n}.$$

Plugging $\sigma_k(\mathbf{A}_{1,1:k}) \geq (1 - \varepsilon)^2$ into (14), we have

$$\sin^2 \varphi_{1,k,k} - \sin^2 \theta_k \leq \max_{\mathbf{x} \in \mathbf{S}^{k-1}} \left[(1 - \varepsilon)^{-2} \left\| \mathbf{P}_{\mathcal{Y}_2^\perp} (\mathbf{A}_{1,1:k} \mathbf{x}) \right\|^2 - \left\| \mathbf{P}_{\mathcal{X}_2^\perp} (\mathbf{U}_{1,1:k} \mathbf{x}) \right\|^2 \right].\quad (15)$$

Notice that the RHS of (15) is equal to

$$\mathbf{x}^\top \left((1 - \varepsilon)^{-2} \mathbf{A}_{1,1:k}^\top \mathbf{P}_{\mathcal{Y}_2^\perp} (\mathbf{A}_{1,1:k}) - \mathbf{U}_{1,1:k}^\top \mathbf{P}_{\mathcal{X}_2^\perp} (\mathbf{U}_{1,1:k}) \right) \mathbf{x}.$$

Following a standard covering argument (Appendix F), we can evaluate the RHS of (15) by calculating on a $\frac{1}{4}$ -net \mathcal{N} .

$$\sin^2 \varphi_{1,k,k} - \sin^2 \theta_k \leq 2 \max_{\mathbf{x} \in \mathcal{N}} \left[(1 - \varepsilon)^{-2} \left\| \mathbf{P}_{\mathcal{Y}_2^\perp} (\mathbf{A}_{1,1:k} \mathbf{x}) \right\|^2 - \left\| \mathbf{P}_{\mathcal{X}_2^\perp} (\mathbf{U}_{1,1:k} \mathbf{x}) \right\|^2 \right].\quad (16)$$

Now it suffices to bound the maximum of the last quantity over the $\frac{1}{4}$ -net \mathcal{N} . We only need to consider the upper bound of the bracket expression for any given $\mathbf{x} \in \mathcal{N}$. Noticing that $\mathbf{A}_{1,1:k} \mathbf{x} = \Phi \mathbf{U}_{1,1:k} \mathbf{x}$ is embedded from $\mathbf{U}_{1,1:k} \mathbf{x}$, the bracket expression is similar to the distortion of $\mathbf{P}_{\mathcal{X}_2^\perp} \mathbf{U}_{1,1:k} \mathbf{x}$ after random embedding, which is given by the following Lemma.

Lemma 6. (Xu et al. (2019), Lemma 2) Suppose Φ is a random matrix with JL property. Suppose \mathbf{x}_1 , \mathcal{X}_2 are respectively a vector and a d -dimensional subspace of \mathbb{R}^N . Denote $\mathbf{y}_1 := \Phi \mathbf{x}_1 / \|\Phi \mathbf{x}_1\|$ and \mathcal{Y}_2 as the projection of \mathcal{X}_2 with Φ . Then there exist universal positive constants c_1, c_2 , for any $\varepsilon \in (0, 1/2)$ and any $n > c_1 \varepsilon^{-2} d$, we have

$$\left| \left\| \mathbf{P}_{\mathcal{Y}_2^\perp}(\mathbf{y}_1) \right\|^2 - \left\| \mathbf{P}_{\mathcal{X}_2^\perp}(\mathbf{x}_1) \right\|^2 \right| \leq \varepsilon \left\| \mathbf{P}_{\mathcal{X}_2^\perp}(\mathbf{x}_1) \right\|^2$$

with probability at least $1 - e^{-c_2 \varepsilon^2 n}$.

To use Lemma 6, we need to reformulate (16) as below.

$$\begin{aligned} & \left| (1 - \varepsilon)^{-2} \left\| \mathbf{P}_{\mathcal{Y}_2^\perp}(\mathbf{A}_{1,1:k} \mathbf{x}) \right\|^2 - \left\| \mathbf{P}_{\mathcal{X}_2^\perp}(\mathbf{U}_{1,1:k} \mathbf{x}) \right\|^2 \right| \\ &= \left\| \mathbf{A}_{1,1:k} \mathbf{x} \right\|^2 \left| (1 - \varepsilon)^{-2} \left\| \mathbf{P}_{\mathcal{Y}_2^\perp} \left(\frac{\mathbf{A}_{1,1:k} \mathbf{x}}{\|\mathbf{A}_{1,1:k} \mathbf{x}\|} \right) \right\|^2 - \left\| \mathbf{A}_{1,1:k} \mathbf{x} \right\|^{-2} \left\| \mathbf{P}_{\mathcal{X}_2^\perp}(\mathbf{U}_{1,1:k} \mathbf{x}) \right\|^2 \right| \\ &\leq (1 + \varepsilon)^2 \left| (1 - \varepsilon)^{-2} \left\| \mathbf{P}_{\mathcal{Y}_2^\perp} \left(\frac{\mathbf{A}_{1,1:k} \mathbf{x}}{\|\mathbf{A}_{1,1:k} \mathbf{x}\|} \right) \right\|^2 - \left\| \mathbf{A}_{1,1:k} \mathbf{x} \right\|^{-2} \left\| \mathbf{P}_{\mathcal{X}_2^\perp}(\mathbf{U}_{1,1:k} \mathbf{x}) \right\|^2 \right|. \end{aligned} \quad (17)$$

Now we can invoke Lemma 6 and get

$$\begin{aligned} & \left| (1 - \varepsilon)^{-2} \left\| \mathbf{P}_{\mathcal{Y}_2^\perp} \left(\frac{\mathbf{A}_{1,1:k} \mathbf{x}}{\|\mathbf{A}_{1,1:k} \mathbf{x}\|} \right) \right\|^2 - \left\| \mathbf{A}_{1,1:k} \mathbf{x} \right\|^{-2} \left\| \mathbf{P}_{\mathcal{X}_2^\perp}(\mathbf{U}_{1,1:k} \mathbf{x}) \right\|^2 \right| \\ &\leq (1 - \varepsilon)^{-2} \left| \left\| \mathbf{P}_{\mathcal{Y}_2^\perp} \left(\frac{\mathbf{A}_{1,1:k} \mathbf{x}}{\|\mathbf{A}_{1,1:k} \mathbf{x}\|} \right) \right\|^2 - \left\| \mathbf{P}_{\mathcal{X}_2^\perp}(\mathbf{U}_{1,1:k} \mathbf{x}) \right\|^2 \right| \\ &\quad + \left| (1 - \varepsilon)^{-2} - \left\| \mathbf{A}_{1,1:k} \mathbf{x} \right\|^{-2} \right| \left\| \mathbf{P}_{\mathcal{X}_2^\perp}(\mathbf{U}_{1,1:k} \mathbf{x}) \right\|^2 \end{aligned} \quad (18)$$

$$\begin{aligned} &\leq 4\varepsilon \left\| \mathbf{P}_{\mathcal{X}_2^\perp}(\mathbf{U}_{1,1:k} \mathbf{x}) \right\|^2 + 8\varepsilon \left\| \mathbf{P}_{\mathcal{X}_2^\perp}(\mathbf{U}_{1,1:k} \mathbf{x}) \right\|^2 \\ &= 12\varepsilon \sin^2 \theta_k, \end{aligned} \quad (19)$$

where $\varepsilon < 1/2$ is used implicitly.

Thus, for any $\varepsilon \in (0, 1/2)$, with probability at least $1 - 9^d e^{-c_2 \varepsilon^2 n}$, we have

$$\sin^2 \varphi_{1,k,k} - \sin^2 \theta_k \leq 2 \cdot \frac{9}{4} \cdot 12\varepsilon \sin^2 \theta_k.$$

Redefining $c_1 := \max\{c_1, 2 \ln 9/c_2\}$, $c_2 := (c_2 - \ln 9/c_1)/54^2$, we have (12) hold.

5.3.2 Proof of (13)

In this proof, we follow the same approach as Section 5.3.1. According to (2), we have

$$\begin{aligned} \sin^2 \varphi_{k,d_1,1} &= \min_{\mathbf{x} \in \mathcal{S}^{d_1-k}} \frac{\left\| \mathbf{P}_{\mathcal{Y}_2^\perp}(\mathbf{A}_{1,k:d_1} \mathbf{x}) \right\|^2}{\left\| \mathbf{A}_{1,k:d_1} \mathbf{x} \right\|^2}, \\ \sin^2 \theta_k &= \min_{\mathbf{x} \in \mathcal{S}^{d_1-k}} \left\| \mathbf{P}_{\mathcal{X}_2^\perp}(\mathbf{U}_{1,k:d_1} \mathbf{x}) \right\|^2. \end{aligned}$$

Then we could derive the counterpart of (14), (15), (16), and (17) as below.

$$\begin{aligned}
\sin^2 \varphi_{k,d_1,1} - \sin^2 \theta_k &\geq \min_{\mathbf{x} \in \mathcal{S}^{d_1-k}} \left[\left\| \mathbf{P}_{\mathcal{Y}_2^\perp} \left(\frac{\mathbf{A}_{1,k:d_1} \mathbf{x}}{\|\mathbf{A}_{1,k:d_1} \mathbf{x}\|} \right) \right\|^2 - \left\| \mathbf{P}_{\mathcal{X}_2^\perp} (\mathbf{U}_{1,k:d_1} \mathbf{x}) \right\|^2 \right] \\
&= - \max_{\mathbf{x} \in \mathcal{S}^{d_1-k}} \left[\left\| \mathbf{P}_{\mathcal{X}_2^\perp} (\mathbf{U}_{1,k:d_1} \mathbf{x}) \right\|^2 - \left\| \mathbf{P}_{\mathcal{Y}_2^\perp} \left(\frac{\mathbf{A}_{1,k:d_1} \mathbf{x}}{\|\mathbf{A}_{1,k:d_1} \mathbf{x}\|} \right) \right\|^2 \right] \\
&\geq - \max_{\mathbf{x} \in \mathcal{S}^{d_1-k}} \left[\left\| \mathbf{P}_{\mathcal{X}_2^\perp} (\mathbf{U}_{1,k:d_1} \mathbf{x}) \right\|^2 - (1+\varepsilon)^{-2} \left\| \mathbf{P}_{\mathcal{Y}_2^\perp} (\mathbf{A}_{1,k:d_1} \mathbf{x}) \right\|^2 \right] \\
&\geq -2 \max_{\mathbf{x} \in \mathcal{N}} \left[\left\| \mathbf{P}_{\mathcal{X}_2^\perp} (\mathbf{U}_{1,k:d_1} \mathbf{x}) \right\|^2 - (1+\varepsilon)^{-2} \left\| \mathbf{P}_{\mathcal{Y}_2^\perp} (\mathbf{A}_{1,k:d_1} \mathbf{x}) \right\|^2 \right] \\
&\geq -2(1+\varepsilon)^2 \max_{\mathbf{x} \in \mathcal{N}} \left[\frac{\left\| \mathbf{P}_{\mathcal{X}_2^\perp} (\mathbf{U}_{1,k:d_1} \mathbf{x}) \right\|^2}{\|\mathbf{A}_{1,k:d_1} \mathbf{x}\|^2} - (1+\varepsilon)^{-2} \left\| \mathbf{P}_{\mathcal{Y}_2^\perp} \left(\frac{\mathbf{A}_{1,k:d_1} \mathbf{x}}{\|\mathbf{A}_{1,k:d_1} \mathbf{x}\|} \right) \right\|^2 \right],
\end{aligned} \tag{20}$$

where \mathcal{N} here denotes the $\frac{1}{4}$ -net of \mathcal{S}^{d_1-k} .

Now we consider each given $\mathbf{x} \in \mathcal{N}$. We could derive the counterpart of (18) and (19) as below

$$\begin{aligned}
&\left| \frac{\left\| \mathbf{P}_{\mathcal{X}_2^\perp} (\mathbf{U}_{1,k:d_1} \mathbf{x}) \right\|^2}{\|\mathbf{A}_{1,k:d_1} \mathbf{x}\|^2} - (1+\varepsilon)^{-2} \left\| \mathbf{P}_{\mathcal{Y}_2^\perp} \left(\frac{\mathbf{A}_{1,k:d_1} \mathbf{x}}{\|\mathbf{A}_{1,k:d_1} \mathbf{x}\|} \right) \right\|^2 \right| \\
&\leq ((1-\varepsilon)^{-2} - (1+\varepsilon)^{-2}) \left\| \mathbf{P}_{\mathcal{X}_2^\perp} (\mathbf{U}_{1,k:d_1} \mathbf{x}) \right\|^2 + (1+\varepsilon)^{-2} \left\| \mathbf{P}_{\mathcal{X}_2^\perp} (\mathbf{U}_{1,k:d_1} \mathbf{x}_1) \right\|^2 \varepsilon \\
&\leq 9\varepsilon \sin^2 \theta_k.
\end{aligned}$$

Following the same argument as the end of Section 5.3.1, we could complete the proof.

5.4 Proof of Theorem 2

According to Section 5.1, it suffices to prove Theorem 2 with $L = 2$. For convenience, we also use θ_k (resp. ψ_k) instead of $\theta_k^{1,2}$ (resp. $\psi_k^{1,2}$) to denote the k -th (resp. embedded) canonical angle. Then we only need to prove

$$(1-\varepsilon)\theta_k \leq \psi_k \leq (1+\varepsilon)\theta_k, \quad \forall 1 \leq k \leq d_1. \tag{21}$$

According to Lemma 4, for any $\delta \in (0, 1/2)$, there exist universal positive constants c_1, c_2 , such that for any $n > c_1 \delta^{-2} d$, with probability at least $1 - e^{-c_2 \delta^2 n}$, we have

$$(1-\delta)\sin \theta_k \leq \sin \psi_k \leq (1+\delta)\sin \theta_k.$$

We consider two cases: $\theta_k \in [0, \pi/4]$ and $\theta_k \in [\pi/4, \pi/2]$. When $\theta_k \in [0, \pi/4]$, we have

$$\begin{aligned} |\psi_k - \theta_k| &\leq |\arcsin((1 \pm \delta) \sin \theta_k) - \arcsin(\sin \theta_k)| \\ &\leq \frac{\delta \sin \theta_k}{\sqrt{1 - \xi_k^2}}, \end{aligned}$$

where the last inequality is because of Mean Value Theorem and $(1 - \delta) \sin \theta_k < \xi_k < (1 + \delta) \sin \theta_k$. Assume $\delta \leq 1/3$, we have

$$\begin{aligned} |\psi_k - \theta_k| &\leq \frac{\delta \sin \theta_k}{\sqrt{1 - (1 + \delta)^2 \sin^2 \theta_k}} \\ &\leq \frac{\delta \sin \theta_k}{\sqrt{1 - (4/3)^2 \sin^2 \theta_k}} \\ &\leq 3\delta\theta_k. \end{aligned}$$

When $\theta_k \in [\pi/4, \pi/2]$, considering that the function \arcsin is uniformly continuous within interval $[1/2, 1]$, for any $\epsilon \in (0, 1/2)$, there exists constant $\delta_\epsilon > 0$, such that for any $|\sin \psi_k - \sin \theta_k| < \delta_\epsilon$, we have

$$|\theta_k - \psi_k| \leq \epsilon \leq \epsilon\theta_k.$$

Redefining $\varepsilon := \max\{\epsilon, 3\delta\}$, we can get (21).

One should note that in the second case, i.e., $\theta_k \in [\pi/4, \pi/2]$, we fail to prove the embedded dimension $n = O(\varepsilon^{-2})$. To get this conclusion, we need to first prove

$$|\cos^2 \psi_k - \cos^2 \theta_k| \leq C_1 \varepsilon \cos \theta_k + C_2 \varepsilon^2,$$

and then use the arccos function to get this result. Since the proof is similar with that of Lemma 4, we postpone it to Appendix B.

6 Compressed Subspace Learning: Applications

In this section, we will show instances of this framework on three subspace-related tasks, namely, subspace visualization, active subspace detection, and subspace clustering. It is empirically verified that random projection with partial Fourier matrices can significantly reduce the computational complexity, without deteriorating performance. The related theoretical analyses are deferred to appendix. For convenience, we call the algorithm with JL random projection as the compressed version, such as compressed subspace clustering. Throughout this section, we denote the number of samples as M .

6.1 Datasets

We will use the following two real-world datasets to test the performance of Algorithm 1.

YaleB Face dataset consists of frontal face images of 38 human subjects under 64 different illumination conditions. The size of images is 192×168 . We reshape each image to a vector of 32256 dimensions. It is assumed that images of the same subject lie in a 9-dimensional subspace (Wang and Yu, 2016). For convenience, in the following experiments, we randomly select 4 subjects to analyze their face images.

Webb Spam Corpus 2011 dataset is a collection of approximately 350,000 spam web pages, which are divided into two categories. The feature is extracted following the way in LIBSVM², and its dimension is over 1.6 million. In the following experiments, we uniformly sample 1000 data points within each category, and model them with UoS. Specifically, we assume that data points belonging to the same category lie in the same 10-dimensional subspace³. We remark that applying subspace learning algorithms on this dataset directly is infeasible. One reason is that the 2000 samples occupies 230GB, and it is impossible to be saved in the memory of any general personal computer.⁴ Under such circumstance, dimensionality is not only beneficial, but also necessary.

6.2 Compressed Subspace Visualization

Data visualization is an effective way to help people understand high-dimensional data. Different from 3-dimensional space, data in high-dimensional space can not be depicted directly in plot, which brings difficulty in the direct understanding. Data visualization refers to representing data in a visual context to help people quickly capture the main relationship between data points, and acquire enough information.

Subspace visualization is designed for UoS model. One method proposed in Shen et al. (2018) is based on canonical angles, and thus called angle-based subspace visualization. This method often suffers from the curse of dimensionality, in that the visualized data is often of high dimension. To handle this problem, we design the compressed angle-based subspace visualization algorithm as per the Algorithm 1, and test its performance on two real-world datasets, i.e., YaleB Face dataset and Webb Spam Corpus 2011 dataset. The experimental results are shown in Figure 2(a) and (b). The implementation details are postponed to Appendix C.1.

²<https://www.csie.ntu.edu.tw/~cjlin/libsvmtools/datasets/binary.html>

³The dimension of subspace is assumed to be ten because the energy for these two categories on the first 10 principal components account for 42.7% and 32.9%.

⁴An alternative way is to save data on external storage, and only save recently-used data in memory. However, such method will definitely increase the time consumption because reading the storage takes hundreds of times more time than reading the memory.

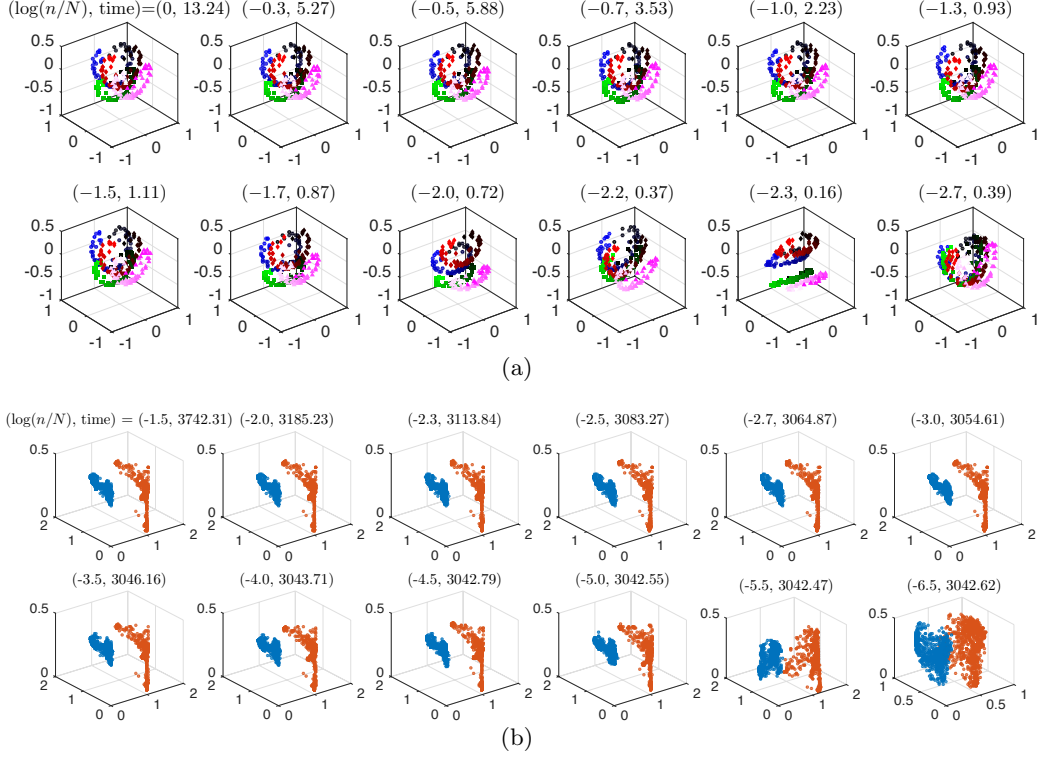


Figure 2: Compressed angle-based subspace visualization results and running time under different embedded dimensions n on (a) YaleB Face dataset and (b) Webb Spam Corpus 2011 dataset. Different colors represent various categories. The running time is in second.

According to Figure 2(a), the visualization result changes very slightly with the embedded dimension as long as the compression ratio exceeds $2E-2$. This indicates that proper compression does not bring great distortion to the visualization result, but greatly reduces the time consumption. Similar phenomena are observed in Figure 2(b). We make two additional remarks for this figure. First, for Webb Spam Corpus 2011 dataset, the extremely high dimension prevents us from obtaining the visualization result of original dataset. We can only infer that it can be well approximated by the results under $n/N \geq 1E-5$. The principle behind such inference is deferred to Theorem 4, in Appendix C.1. Second, though the direct application of subspace visualization on the original dataset is infeasible, the compressed version of this algorithm yields a satisfactory result.

6.3 Compressed Active Subspace Detection

Active subspace detection refers to identifying which subspace the observed data belongs to, when all candidate subspaces are known. This problem is often encountered in radar target detection, user detection in wireless network, and image-based verification of employees (Lodhi and Bajwa, 2018). A typical algorithm is the Maximum Likelihood (ML), the

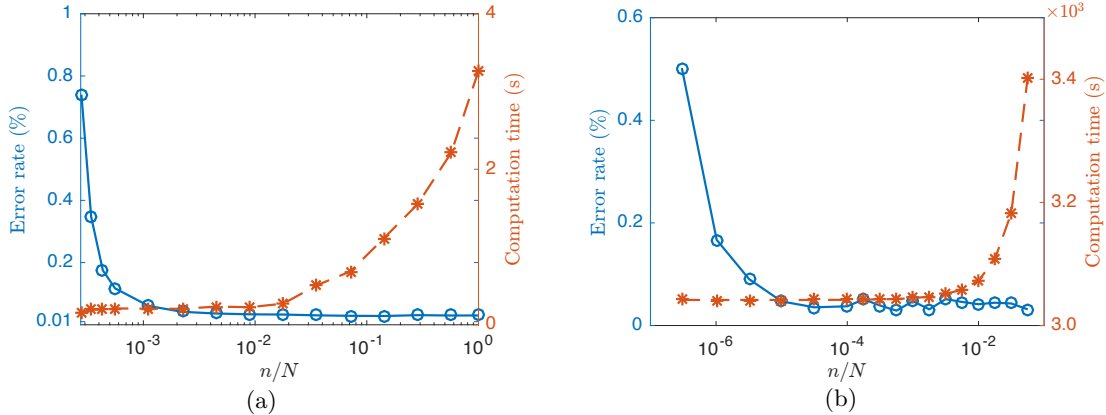


Figure 3: The error rate and running time of compressed ML algorithm under different embedded dimensions n on (a) YaleB Face dataset and (b) Webb Spam Corpus 2011 dataset. The results have been averaged over 5 random trials.

computational complexity of which increases linearly with the dimension of data. We design the compressed ML algorithm as per the Algorithm 1. The implementation details and the performance analysis is deferred to Definition 5 and Theorem 5, respectively, in Appendix C.2.

We apply compressed ML for active subspace detection on two real-world datasets, and plot the experimental results in Figure 3(a) and (b). It is observed that the compressed ML for active subspace detection allows for compression ratio as low as $n/N = 1\text{E}-2$ and $1\text{E}-4$ on these two datasets, respectively. In other words, the detection accuracy is kept at a very low level as long as the compression ratio is higher than this number, but the detection time becomes much fewer than the original algorithm. This verifies the effectiveness of JL random projection. Another observation is that when we classify Web Spam Corpus 2011 dataset with compressed ML algorithm for active subspace detection, a low error rate is obtained, which suggests that the UoS model fits this dataset well.

6.4 Compressed Subspace Clustering

Subspace clustering seeks to find clusters in different subspaces within a dataset. Many algorithms are proposed to solve this problem, and Sparse Subspace Clustering (SSC) is one of the most popular methods for its high accuracy. However, this method also undergoes the high computational complexity when data dimension is high.

To handle this problem, compressed SSC is proposed (Mao and Gu, 2014), which is subsumed in Algorithm 1. We test its performance on two real-world datasets and the results are shown in Figure 4(a) and (b). With the decrease of compression ratio, the running time drops greatly, while the low error rate is kept.

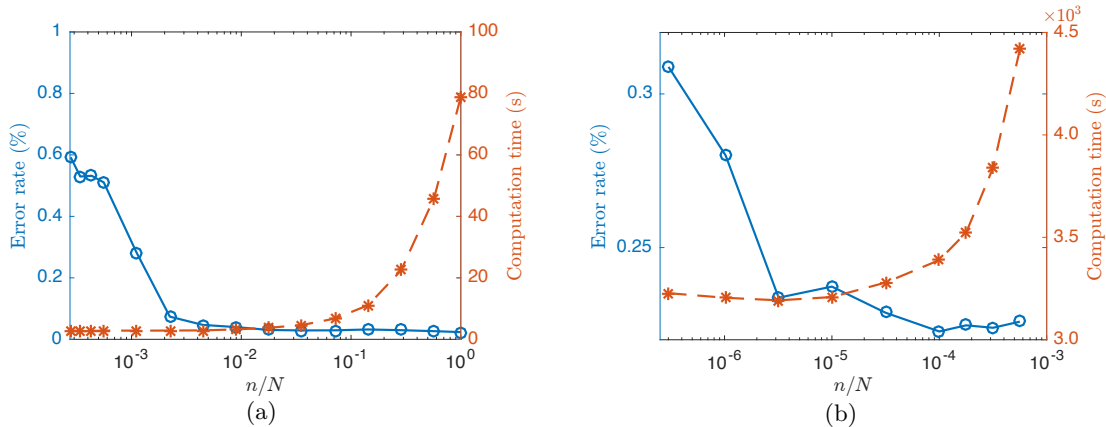


Figure 4: The error rate and running time of compressed Sparse Subspace Clustering under different compressed dimensions n on (a) YaleB Face dataset and (b) Webb Spam Corpus 2011 dataset. The results has been averaged over 10 random trials for (a) and 5 random trials for (b).

We conclude this section with a final remark that the subspace clustering algorithm studied here has been widely investigated. Mao and Gu (2014) and Wang et al. (2019) adopt various types of random projections as dimensionality reduction methods, and apply subspace clustering on the compressed dataset to reduce computational burden. Heckel et al. (2015) analyzes the performance of SSC, TSC, and SSC-OMP when applied to compressed dataset, under the assumption that the random matrices have RIP for points on union of subspaces. Meng et al. (2018) proposes a general framework capable of analyzing the performance of various compressed subspace clustering algorithms, as long as the random matrix has affinity preserving property. In this work, Theorem 3 indicates that JL random projection approximately preserves subspace affinity. By using this theorem in conjunction with the analysis in Meng et al. (2018), we can provide theoretical performance guarantee for the compressed sparse subspace clustering algorithm presented in this section.

7 Conclusion

In this work, we unveiled the subspace structure preserving property of JL random projection. Here the subspace structure is described in terms of canonical angles, which have the best characterization of relative subspace positions. Specifically, it is proved that for a finite collection of L subspaces, with probability $1 - \delta$, each canonical angle between any two subspaces is preserved up to $(1 \pm \varepsilon)$ when the dimension is reduced to $n = O(\varepsilon^{-2} \max\{d, \ln L, \ln(1/\delta)\})$. This main theoretical conclusion is called CAP property. Based on this result, we established a general subspace RIP, which describes the ability to

preserve subspace distance of JL random projection. We say it is *general* because it works for almost arbitrary notion of subspace distance.

Inspired by the above theoretical discovery, we proposed the CSL framework. This framework enables to process data lying on UoS in a space with dimension much lower than the ambient dimension of the data. This was achieved by safely mapping the data to a space with dimension in the same order of subspace dimensions, which is generally much lower than the ambient dimension, via JL random projection. This dimensionality reduction step reduces the time consumption and memory requirement of many UoS-based algorithms. To show the power of CSL framework, we took three subspace learning tasks, namely subspace visualization, active subspace detection, and subspace clustering, as examples. We empirically verified the efficiency and practicability of CSL framework when applied on these three tasks, and theoretically analyzed the performance degradation caused by JL random projection based on CAP property. Considering that our theory is not constrained to specific algorithms, the extension to other subspace learning tasks is possible.

A Canonical Angles and Subspace Distances

We have emphasized that canonical angles better characterize the relative subspace positions than single subspace distance. We take the following example to support this. Considering the three two-dimensional subspaces in \mathbb{R}^4 ,

$$\begin{aligned}\mathcal{S}_1 &:=\text{span}([1, 0, 0, 0]^T, [0, 1, 0, 0]^T), \\ \mathcal{S}_2 &:=\text{span}([1, 0, 0, 0]^T, [0, 0, 1, 0]^T), \\ \mathcal{S}_3 &:=\text{span}([1, 0, 1, 0]^T, [0, 1, 0, 1]^T),\end{aligned}$$

it is obvious that the relative position between \mathcal{S}_1 and \mathcal{S}_2 differs from that between \mathcal{S}_1 and \mathcal{S}_3 , for that \mathcal{S}_1 and \mathcal{S}_2 intersect, while \mathcal{S}_1 and \mathcal{S}_3 do not. Such difference can be visualized by projecting the unit circle in \mathcal{S}_2 and \mathcal{S}_3 onto \mathcal{S}_1 , as shown in Figure 5. However, such difference cannot be reflected by projection Frobenius-norm distance, because it equals to 1 whether when we measure \mathcal{S}_1 and \mathcal{S}_2 or \mathcal{S}_1 and \mathcal{S}_3 . Other notions of subspace distance have similar problems.

The advantage of canonical angles in the ability to describe relative subspace positions is also shown by the fact that any notion of rotation-invariant subspace distance is a function of canonical angles. Rotation-invariant is a natural requirement for distances and is widely satisfied. We present a list of well-known notions of subspace distance and their dependence on canonical angles in Table 1, where d denotes the dimension of subspaces \mathcal{X}_1 , \mathcal{X}_2 , and $\theta_1 \leq \dots \leq \theta_d$ denote the canonical angles. The extension of some notions of distance are listed in Table 2 for subspaces with different dimensions $d_1 < d_2$ (Ye and Lim, 2016).

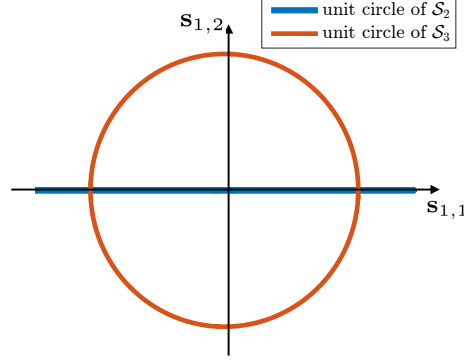


Figure 5: The projection of unit circles in \mathcal{S}_2 and \mathcal{S}_3 onto subspace \mathcal{S}_1 . The x - and y -axis represents the projection onto two base vectors of \mathcal{S}_1 , i.e., $\mathbf{s}_{1,1} := [1, 0, 0, 0]$, $\mathbf{s}_{1,2} := [0, 1, 0, 0]$, respectively.

Table 1: Some definitions of distance between subspaces

projection F-norm	$d_0^\kappa(\mathcal{X}_1, \mathcal{X}_2) := \left(\sum_{k=1}^d \sin^2 \theta_k \right)^{1/2}$
Fubini-Study	$d_0^\phi(\mathcal{X}_1, \mathcal{X}_2) := \cos^{-1} \left(\prod_{k=1}^d \cos \theta_k \right)$
Grassmann	$d_0^G(\mathcal{X}_1, \mathcal{X}_2) := \left(\sum_{k=1}^d \theta_k^2 \right)^{1/2}$
Binet-Cauchy	$d_0^\beta(\mathcal{X}_1, \mathcal{X}_2) := \left(1 - \prod_{k=1}^d \cos^2 \theta_k \right)^{1/2}$
Procrustes	$d_0^\rho(\mathcal{X}_1, \mathcal{X}_2) := 2 \left(\sum_{k=1}^d \sin^2 (\theta_k/2) \right)^{1/2}$
Asimov	$d_0^\alpha(\mathcal{X}_1, \mathcal{X}_2) := \theta_d$
Spectral	$d_0^\sigma(\mathcal{X}_1, \mathcal{X}_2) := 2 \sin (\theta_d/2)$
Projection	$d_0^\pi(\mathcal{X}_1, \mathcal{X}_2) := \sin \theta_d$

Due to the powerful characterization of canonical angles, the analyses on the distortion of the above subspace distances are unified by CAP property. It is provable that all notions of distance in Table 1 and 2 are Lipschitz continuous and satisfy (5). By Theorem 3, all of these distances are approximately preserved by JL random projection.

It is sometimes useful to have different notions of subspace distance for specific applications. The projection Frobenius-norm distance is also called chordal distance. It is widely used in the subspace quantization problem appearing in the precoding of multiple-antenna wireless systems (Love and Heath, 2005a). The Fubini-Study distance is also investigated in this problem (Love and Heath, 2005b). The Grassmann distance is the geodesic distance when viewing subspaces as points on the Grassmannian manifold, i.e., it can be locally interpreted as the shortest length of all curves between the two measured subspaces on manifold. It can be used to assess the convergence of the Riemann-Newton method (Ab-

Table 2: Some generalized definitions of distance on subspace with different dimensions

projection F-norm	$d^\kappa(\mathcal{X}_1, \mathcal{X}_2) := \left((d_2 - d_1)/2 + \sum_{k=1}^{d_1} \sin^2 \theta_k \right)^{1/2}$
Grassmann	$d^G(\mathcal{X}_1, \mathcal{X}_2) := \left((d_2 - d_1) \pi^2/4 + \sum_{k=1}^{d_1} \theta_k^2 \right)^{1/2}$
Procrustes	$d^\rho(\mathcal{X}_1, \mathcal{X}_2) := \left(d_2 - d_1 + 2 \sum_{k=1}^{d_1} \sin^2(\theta_k/2) \right)^{1/2}$

sil et al., 2004). Both Binet-Cauchy and the projection Frobenius-norm distance are used in some subspace learning algorithms for the positive definiteness of the kernel they are induced from Hamm and Lee (2008). Definitions determined by single canonical angle, such as the Asimov distance, the spectral distance, and the projection distance, share the advantage of being more robust to noise.

B Supplement for the Proof of Theorem 2

To establish $n = O(\varepsilon^{-2})$ for $\theta \in [\pi/4, \pi/2]$, we will first prove

$$|\cos^2 \psi_k - \cos^2 \theta_k| \leq C_1 \varepsilon \cos \theta_k + C_2 \varepsilon^2, \quad (22)$$

where C_1, C_2 are universal constants, and then derive the relationship between n and ε .

To prove (22), according to Lemma 3, it suffices to prove

$$\begin{aligned} P(\cos^2 \varphi_{1,k,k} - \cos^2 \theta_k \leq C_1 \varepsilon \cos \theta_k + C_2 \varepsilon^2) &\geq 1 - e^{-c_2 \varepsilon^2 n}, \\ P(\cos^2 \theta_k - \cos^2 \varphi_{k,d_1,1} \leq C_1 \varepsilon \cos \theta_k + C_2 \varepsilon^2) &\geq 1 - e^{-c_2 \varepsilon^2 n}. \end{aligned}$$

Proofs of these two inequalities are similar with the argument in Section 5.3.1 and 5.3.2. Readers only need to replace Lemma 6 with the following lemma implied in Xu et al. (2019).

Lemma 7. Suppose Φ is a random matrix with JL property. Suppose $\mathbf{x}_1, \mathcal{X}_2$ are respectively a vector and a d -dimensional subspace in \mathbb{R}^N . Denote $\mathbf{y}_1 := \Phi \mathbf{x}_1 / \|\Phi \mathbf{x}_1\|$ and \mathcal{Y}_2 as the projection of \mathcal{X}_2 with Φ . Then there exist universal positive constants c_1, c_2 , for any $\varepsilon \in (0, 1/2)$ and any $n > c_1 \varepsilon^{-2} d$, we have

$$\left| \|\mathbf{P}_{\mathcal{Y}_2}(\mathbf{y}_1)\|^2 - \|\mathbf{P}_{\mathcal{X}_2}(\mathbf{x}_1)\|^2 \right| \leq C_1 \varepsilon \|\mathbf{P}_{\mathcal{X}_2}(\mathbf{x}_1)\| + C_2 \varepsilon^2 \quad (23)$$

with probability at least $1 - e^{-c_2 \varepsilon^2 n}$.

Proof. The proof follows from Xu et al. (2019), Lemma 2. \square

According to (22), when $\cos \theta_k \leq \varepsilon$, we could immediately get

$$|\cos \psi_k - \cos \theta_k| \leq C_0 \varepsilon \quad (24)$$

with probability at least $1 - e^{-c_2\varepsilon^2n}$, where C_0 is a positive universal constant. When $\cos \theta_k > \varepsilon$, we have

$$|\cos \psi_k - \cos \theta_k| = \frac{|\cos^2 \psi_k - \cos^2 \theta_k|}{\cos \psi_k + \cos \theta_k} \leq C_1\varepsilon + C_2\varepsilon. \quad (25)$$

From (24) and (25), recalling that $\theta \in [\pi/4, \pi/2]$, we could prove

$$\psi_k - \theta_k \leq C\varepsilon\theta_k,$$

where C is a positive universal constant and thus $n = O(\varepsilon^2)$.

C Supplement for Section 6

In this section, we will introduce implementation details of two compressed algorithms, namely compressed angle-based subspace visualization and compressed ML for active subspace detection, and theoretically analyze their performance distortion. We follow the notations from Section 6.

C.1 Compressed Subspace Visualization

We first review the angle-based subspace visualization algorithm proposed in Shen et al. (2018). It takes data points $\mathbf{x}_1, \dots, \mathbf{x}_M$ as input, which lie on L subspaces $\mathcal{X}_1, \dots, \mathcal{X}_L$. The labels of data and the bases of L subspaces are assumed to be known. The algorithm first constructs a dissimilarity matrix \mathbf{D} , and then embeds the data into a 2- or 3-dimensional space via MDS. The dissimilarity matrix $\mathbf{D} := (D_{i,j})_{i,j}$ is defined as below.

$$D_{\text{SV}}(\mathbf{x}_i, \mathbf{x}_j) = \begin{cases} \sin^2 \theta^{i,j}, & \mathbf{x}_i, \mathbf{x}_j \text{ lie in the same subspace;} \\ \left(v \sin \theta^{i,j} + u \min_k (\sin \tilde{\theta}^{i,k} + \sin \tilde{\theta}^{j,k}) \right)^2, & \text{otherwise;} \end{cases} \quad (26)$$

where $\theta^{i,j}$ denotes the canonical angle between \mathbf{x}_i and \mathbf{x}_j , and $\tilde{\theta}^{i,k}$ denotes the canonical angle between \mathbf{x}_i and \mathcal{X}_k . u, v denote two algorithmic parameters, which balance the term $\sin \theta^{i,j}$ and $\min_k (\sin \tilde{\theta}^{i,k} + \sin \tilde{\theta}^{j,k})$. The second step MDS is completed by applying eigenvalue decomposition on double-centered distance matrix

$$\mathbf{B} := -\frac{1}{2}\mathbf{H}\mathbf{D}\mathbf{H}, \quad (27)$$

and obtain eigenvectors $\mathbf{v}_1, \mathbf{v}_2$ (or $\mathbf{v}_1, \mathbf{v}_2, \mathbf{v}_3$) corresponding to the largest two (or three) eigenvalues $\lambda_1 \geq \lambda_2$ (or $\lambda_1 \geq \lambda_2 \geq \lambda_3$), where $\mathbf{H} := \mathbf{I} - 1/M\mathbf{1}\mathbf{1}^T$ is the centering matrix and $\mathbf{1} \in \mathbb{R}^M$ denotes all-ones vector. The output coordinate matrix is denoted by $\mathbf{C} = [\lambda_1^{1/2}\mathbf{v}_1, \lambda_2^{1/2}\mathbf{v}_2]$ (or $\mathbf{C} = [\lambda_1^{1/2}\mathbf{v}_1, \lambda_2^{1/2}\mathbf{v}_2, \lambda_3^{1/2}\mathbf{v}_3]$).

According to Algorithm 1, we design compressed angle-based subspace visualization algorithm as below.

Definition 3. There are three steps to implement compressed angle-based subspace visualization algorithm. 1. Embedding data $\mathbf{x}_i \in \mathbb{R}^N$ with a partial Fourier matrix and getting the embeded data \mathbf{y}_i . 2. Calculating dissimilarity matrix $\hat{\mathbf{D}}$ by using \mathbf{y}_i . 3. Applying MDS and returning output coordinate matrix $\hat{\mathbf{C}}$.

The following theorem states the error introduced by replacing \mathbf{D} with $\hat{\mathbf{D}}$.

Theorem 4. Suppose there are M data points in \mathbb{R}^N , lying on L subspaces with dimensions no more than d . The dissimilarity matrix constructed according to (26) is denoted as $\mathbf{D} \in \mathbb{R}^{M \times M}$. The output coordinate matrix is denoted as $\mathbf{C} \in \mathbb{R}^{M \times 2}$. After applying random projection with partial Fourier matrices, we get M compressed data points in \mathbb{R}^n . The corresponding dissimilarity matrix and coordinate matrix is denoted as $\hat{\mathbf{D}}$ and $\hat{\mathbf{C}}$, respectively. Assume the eigenvalue of double-centered matrix \mathbf{B} defined in (27) satisfies $\lambda_1 > \lambda_2 > \lambda_3 \geq \dots \geq \lambda_M$.⁵ For any $\varepsilon \in (0, 1)$, there exist two universal positive constants c_1, c_2 , such that for any $n \geq c_1 \varepsilon^{-2} \max\{d, \ln(M+L)\}$, with probability at least $1 - e^{-c_2 \varepsilon^2 n}$, we have

$$\left\| \hat{\mathbf{C}} - \mathbf{C} \right\|_F^2 \leq 2 \|\mathbf{D}\|_F \varepsilon + \frac{4 \|\mathbf{D}\|_F^2 \lambda_1}{(\lambda_1 - \lambda_2)^2} \varepsilon^2 + \frac{4 \|\mathbf{D}\|_F^2 \lambda_2}{\min\{(\lambda_1 - \lambda_2)^2, (\lambda_2 - \lambda_3)^2\}} \varepsilon^2. \quad (28)$$

Proof. The proof is postponed to Appendix D. \square

By (28), we have $\|\hat{\mathbf{C}} - \mathbf{C}\|_F^2 \leq 2\|\mathbf{D}\|_F \varepsilon + o(\varepsilon)$. When ε is small, the error in visualization caused by embedding is also small.

Remark 3. The case considered in Theorem 4 is that data points are visualized in a two dimensional plot. When we visualize data points in a three dimensional plot, i.e., take the eigenvectors of \mathbf{B} corresponding to the largest three eigenvalues in MDS step, the visualization error will further increase by

$$\|\mathbf{D}\|_F \varepsilon + \frac{4 \|\mathbf{D}\|_F^2 \lambda_3}{\min\{(\lambda_2 - \lambda_3)^2, (\lambda_3 - \lambda_4)^2\}} \varepsilon^2,$$

under the assumption that $\lambda_3 > \lambda_4$.

C.2 Compressed Active Subspace Detection

Active subspace detection can be mathematically written as the following hypothesis problem.

$$\mathcal{H}_i : \quad \mathbf{x} = \mathbf{U}_i \mathbf{s} + \mathbf{n},$$

⁵The condition that $\lambda_1 \neq \lambda_2 \neq \lambda_3$ is necessary. The reason is that if there exist repeated eigenvalues, the visualization result is not unique. In this case, measuring the distortion caused by embedding becomes ill-defined.

where \mathbf{U}_i denotes the orthonormal basis for the i -th subspace \mathcal{X}_i . Denote $P_{\mathcal{H}_i}(\cdot)$ as the probability conditioned on hypothesis \mathcal{H}_i , and $\bar{\mathcal{H}}_i$ as the event that hypothesis \mathcal{H}_i is accepted. Then $\sum_i^L (1 - P_{\mathcal{H}_i}(\bar{\mathcal{H}}_i))$ is defined as the error rate, which is what we are interested in.

The Maximum Likelihood (ML) method for active subspace detection follows that

$$\bar{i} := \arg \max_{1 \leq i \leq L} \|\mathbf{U}_i^T \mathbf{x}\|. \quad (29)$$

The dependence of ML's correct probability on canonical angles is revealed in Lodhi and Bajwa (2018). In order to show such relation more clearly and quantitatively, we consider random signals instead of determined signals and re-derive such relation. In particular, we first give the definition of affinity in terms of canonical angles, and then show how affinity influences the performance of ML algorithm for active subspace detection.

Definition 4. (Soltanolkotabi and Candes, 2012) The affinity $\text{aff}(\mathcal{X}_1, \mathcal{X}_2)$ between subspace \mathcal{X}_1 and \mathcal{X}_2 with dimension d is defined as below.

$$\text{aff}^2(\mathcal{X}_1, \mathcal{X}_2) = \sum_{k=1}^d \cos^2 \theta_k,$$

where θ_k denotes the k -th canonical angle.

Lemma 8. Assume that \mathbf{s} follows Gaussian distribution $\mathcal{N}(\mathbf{0}, 1/d_i \mathbf{I})$, and noise \mathbf{n} follows Gaussian distribution $\mathcal{N}(\mathbf{0}, \mathbf{R}_n)$. Denote the maximum eigenvalue of \mathbf{R}_n as δ . We have

$$P_{\mathcal{H}_i}(\bar{\mathcal{H}}_i) \geq 1 - \sum_{j \neq i} \exp\left(-\frac{1}{2} \min\{A, A^2\}\right), \quad (30)$$

where

$$A := \frac{1 - \text{aff}_{ij}^2/d_i - \delta d_j}{4(1 + \text{aff}_{ij}^2/d_i + \delta(d_i + d_j))},$$

and aff_{ij} denotes the affinity between subspace \mathcal{X}_i and \mathcal{X}_j , as defined in Definition 4.

Proof. The proof is postponed to Appendix E. □

We design the compressed ML algorithm for active subspace detection following Algorithm 1 as below.

Definition 5. There are two steps to implement compressed ML algorithm for active subspace detection. 1. Embedding data $\mathbf{x} \in \mathbb{R}^N$ with partial Fourier matrices and getting the compressed data \mathbf{y} . 2. Calculating $\bar{i} := \arg \max_{1 \leq i \leq L} \|\mathbf{V}_i^T \mathbf{y}\|$, where \mathbf{V}_i denotes the orthonormal basis of the i -th embedded subspace.

What follows is the performance analysis of compressed ML for active subspace detection.

Theorem 5. Under the same setting as Lemma 8, in non-noisy case, i.e., $\mathbf{n} = 0$, when we apply compressed ML algorithm for active subspace detection, for any $\varepsilon \in (0, 1/2)$, there exist universal positive constants c_1, c_2, c_3 such that for any $n > c_1 \max\{\varepsilon^{-2}, \delta^{-1}\} \cdot \max\{d, \ln L\}$, the correct probability satisfies

$$P_{\mathcal{H}_i}(\bar{\mathcal{H}}_i) \geq 1 - \sum_{j \neq i} \exp\left(-\frac{1}{2} \min\{B, B^2\}\right) - e^{-c_2 \varepsilon^2 n} - e^{-c_3 \delta n},$$

where

$$B := \frac{1 - \text{aff}_{ij}^2(1 + \varepsilon)/d_i - \delta d_j}{4(1 + \text{aff}_{ij}^2(1 + \varepsilon)/d_i + \delta(d_i + d_j))}.$$

Proof. After embedding, we have $\mathbf{y} = \Phi \mathbf{x} = \Phi \mathbf{U}_i \mathbf{s}$. The singular decomposition gives $\Phi \mathbf{U}_i = \mathbf{V}_i \mathbf{\Lambda}_i \mathbf{Q}_i^T$, then we have

$$\mathbf{y} = \mathbf{V}_i \mathbf{\Lambda}_i \mathbf{Q}_i^T \mathbf{s} = \mathbf{V}_i \mathbf{Q}_i^T \mathbf{s} + \mathbf{V}_i (\mathbf{\Lambda}_i - \mathbf{I}) \mathbf{Q}_i^T \mathbf{s}.$$

Denote $\bar{\mathbf{y}} := \mathbf{V}_i \mathbf{Q}_i^T \mathbf{s}$ and $\mathbf{w} := \mathbf{V}_i (\mathbf{\Lambda}_i - \mathbf{I}) \mathbf{Q}_i^T \mathbf{s}$, we have $\mathbf{y} = \bar{\mathbf{y}} + \mathbf{w}$. In the first item below, we will show that $\bar{\mathbf{y}}$ can be regarded as a signal uniformly distributed within the i -th embedded subspace \mathcal{Y}_i . While in the second item, we will show that with probability at least $1 - e^{-O(\delta)}$, \mathbf{w} can be regarded as Gaussian noise whose covariance matrix satisfies $\lambda_{\max}(\mathbf{R}_w) \leq \delta$.

1) Noticing that \mathbf{V}_i is an orthonormal basis for \mathcal{Y}_i , we have $\bar{\mathbf{y}} \in \mathcal{Y}_i$. Its projection onto \mathcal{Y}_i is $\mathbf{V}_i^T \bar{\mathbf{y}} = \mathbf{Q}_i^T \mathbf{s} \sim \mathcal{N}(\mathbf{0}, 1/d_i \mathbf{I})$.

2) The covariance matrix of noise \mathbf{n} is $1/d_i \mathbf{V}_i (\mathbf{\Lambda}_i - \mathbf{I})^2 \mathbf{V}_i^T$. According to Lemma 5, and noticing that the diagonal entries of $\mathbf{\Lambda}_i$ are singular values of matrix $\Phi \mathbf{U}_i$, we have $\lambda_{\max}(\mathbf{R}_w) \leq \delta$ with probability at least $1 - e^{-c_3 \delta n}$ for any $n > c_1 \delta^{-1} \max\{d, \ln L\}$, where c_1, c_3 are two universal positive constants. Then the compressed setting is similar to the noisy setting, whose correct probability is shown in (30). According to Theorem 2, canonical angles between $\mathcal{Y}_i, \mathcal{Y}_j$ satisfy $\psi_k^{i,j} \geq (1 - \varepsilon) \theta_k^{i,j}$ with overwhelming probability. Replacing $\theta_k^{i,j}$ with $(1 - \varepsilon) \theta_k^{i,j}$ in (30), we complete the proof. \square

It is clear that as long as the embedded dimension n satisfies $n > c_1 \varepsilon^{-2} \max\{d, \ln L\}$, embedding will not bring great degradation to the correct probability $P_{\mathcal{H}_i}(\bar{\mathcal{H}}_i)$ for $i = 1, \dots, L$.

D Proof of Theorem 4

Denote the eigenvectors of double-centered dissimilarity matrix \mathbf{B} defined in (27) as $\mathbf{v}_1, \dots, \mathbf{v}_M$, corresponding to eigenvalues $\lambda_1 > \lambda_2 \geq \lambda_3 \geq \dots \geq \lambda_M$. According to the process of MDS, we have $\mathbf{C} = [\lambda_1^{1/2} \mathbf{v}_1, \lambda_2^{1/2} \mathbf{v}_2]$. The visualization result obtained on compressed

dataset is $\hat{\mathbf{C}} = [\hat{\lambda}_1^{1/2} \hat{\mathbf{v}}_1, \hat{\lambda}_2^{1/2} \hat{\mathbf{v}}_2]$, where $\hat{\mathbf{v}}_1, \hat{\mathbf{v}}_2$ and $\hat{\lambda}_1, \hat{\lambda}_2$ denote the first two eigenvectors and eigenvalues of matrix $\hat{\mathbf{B}} := -1/2\mathbf{H}\hat{\mathbf{D}}\mathbf{H}$, respectively. Then we have

$$\begin{aligned}
\|\mathbf{C} - \hat{\mathbf{C}}\|_F^2 &= \sum_{i=1}^2 \left\| \lambda_i^{1/2} \mathbf{v}_i - \hat{\lambda}_i^{1/2} \hat{\mathbf{v}}_i \right\|^2 \\
&= \sum_{i=1}^2 \left\| \lambda_i^{1/2} \mathbf{v}_i - \lambda_i^{1/2} \hat{\mathbf{v}}_i + \lambda_i^{1/2} \hat{\mathbf{v}}_i - \hat{\lambda}_i^{1/2} \hat{\mathbf{v}}_i \right\|^2 \\
&\leq \sum_{i=1}^2 \left(2 \left\| \lambda_i^{1/2} \mathbf{v}_i - \lambda_i^{1/2} \hat{\mathbf{v}}_i \right\|^2 + 2 \left(\lambda_i^{1/2} - \hat{\lambda}_i^{1/2} \right)^2 \right) \\
&\leq \sum_{i=1}^2 \left(2\lambda_i \|\mathbf{v}_i - \hat{\mathbf{v}}_i\|^2 + 2 \left| \lambda_i - \hat{\lambda}_i \right| \right). \tag{31}
\end{aligned}$$

Next we need to use the following lemma about the perturbation theory of matrix eigenvalues and eigenvectors.

Lemma 9. (simplified from Yu et al. (2014), Theorem 2) Assume matrices $\mathbf{A}, \hat{\mathbf{A}} \in \mathbb{R}^{n \times n}$ are symmetric, with eigenvalues $\lambda_1 \geq \dots \geq \lambda_n$ and $\hat{\lambda}_1 \geq \dots \geq \hat{\lambda}_n$, respectively. Fix $1 \leq i \leq n$ and assume that $\lambda_{i-1} > \lambda_i > \lambda_{i+1}$, where $\lambda_0 := \infty$ and $\lambda_{n+1} := -\infty$. Let \mathbf{v}_i and $\hat{\mathbf{v}}_i$ be the vectors satisfying $\mathbf{A}\mathbf{v}_i = \lambda_i\mathbf{v}_i$ and $\hat{\mathbf{A}}\hat{\mathbf{v}}_i = \hat{\lambda}_i\hat{\mathbf{v}}_i$, respectively, and $\mathbf{v}_i^\top \hat{\mathbf{v}}_i \geq 0$. Then

$$\sin \langle \mathbf{v}_i, \hat{\mathbf{v}}_i \rangle \leq \frac{2 \left\| \hat{\mathbf{A}} - \mathbf{A} \right\|_F}{\min\{\lambda_{i-1} - \lambda_i, \lambda_i - \lambda_{i+1}\}}$$

and

$$\left| \hat{\lambda}_i - \lambda_i \right| \leq \left\| \hat{\mathbf{A}} - \mathbf{A} \right\|_F,$$

where $\langle \mathbf{v}_i, \hat{\mathbf{v}}_i \rangle$ denotes the angle between \mathbf{v}_i and $\hat{\mathbf{v}}_i$.

Denote

$$\mathbf{E} := \hat{\mathbf{B}} - \mathbf{B} = -\frac{1}{2}\mathbf{H}(\hat{\mathbf{D}} - \mathbf{D})\mathbf{H}$$

as the error of centered dissimilarity matrix caused by embedding. According to Lemma 9, we have for $i = 1, 2$,

$$\|\mathbf{v}_i - \hat{\mathbf{v}}_i\|^2 \leq 2 \sin^2 \langle \mathbf{v}_i, \hat{\mathbf{v}}_i \rangle \leq \frac{8 \|\mathbf{E}\|_F^2}{\min\{(\lambda_{i-1} - \lambda_i)^2, (\lambda_i - \lambda_{i+1})^2\}}, \tag{32}$$

$$\left| \hat{\lambda}_i - \lambda_i \right| \leq \|\mathbf{E}\|_F. \tag{33}$$

Now we further simplify the F-norm of \mathbf{E} . Considering that matrix \mathbf{H} is a projection matrix with spectral norm no more than 1, we have

$$\|\mathbf{E}\|_F \leq \frac{1}{2} \left\| \hat{\mathbf{D}} - \mathbf{D} \right\|_F.$$

According to Lemma 4, for any $n \geq c_1 \varepsilon^{-2} \max\{d, \ln(M + L)\}$, with probability at least $1 - e^{-c_2 \varepsilon^2 n}$, we have

$$\left\| \hat{\mathbf{D}} - \mathbf{D} \right\|_F \leq \|\mathbf{D}\|_F \varepsilon,$$

and thus

$$\|\mathbf{E}\|_F \leq \frac{1}{2} \|\mathbf{D}\|_F \varepsilon. \quad (34)$$

Plugging (32), (33), and (34) into (31), we can get (28) and complete the proof.

E Proof of Lemma 8

For any $j \neq i$, denote the principal vectors in \mathcal{X}_j for the subspaces pair \mathcal{X}_i and \mathcal{X}_j as $\tilde{\mathbf{U}}_j$. According to the process of ML method, have

$$\begin{aligned} 1 - P_{\mathcal{H}_i}(\bar{\mathcal{H}}_i) &\leq \sum_{j \neq i} P \left(\left\| \tilde{\mathbf{U}}_i^T \mathbf{U}_i \mathbf{s} + \tilde{\mathbf{U}}_i^T \mathbf{n} \right\|^2 - \left\| \tilde{\mathbf{U}}_j^T \mathbf{U}_i \mathbf{s} + \tilde{\mathbf{U}}_j^T \mathbf{n} \right\|^2 < 0 \right) \\ &= \sum_{j \neq i} P \left(\left\| \tilde{\mathbf{s}} + \tilde{\mathbf{U}}_i^T \mathbf{n} \right\|^2 - \left\| \mathbf{\Lambda}_{ij} \tilde{\mathbf{s}} + \tilde{\mathbf{U}}_j^T \mathbf{n} \right\|^2 < 0 \right), \end{aligned} \quad (35)$$

where $\tilde{\mathbf{s}} := \tilde{\mathbf{U}}_i^T \mathbf{U}_i \mathbf{s}$ is the rotation of \mathbf{s} and it still follows distribution $\mathcal{N}(\mathbf{0}, 1/d_i \mathbf{I})$. We will analyze the item $\left\| \tilde{\mathbf{s}} + \tilde{\mathbf{U}}_i^T \mathbf{n} \right\|^2$ and $\left\| \mathbf{\Lambda}_{ij} \tilde{\mathbf{s}} + \tilde{\mathbf{U}}_j^T \mathbf{n} \right\|^2$ in (35).

For the first item, noticing that $\left\| \tilde{\mathbf{s}} + \tilde{\mathbf{U}}_i^T \mathbf{n} \right\|^2$ with expectation removed is a sub-exponential random variable. We calculate its expectation μ_i and variance proxy σ_i as below (Jiao et al. (2018a), Lemma 1).

$$\mu_i = \mathbb{E} \left[\|\tilde{\mathbf{s}}\|^2 \right] + \mathbb{E} \left[\left\| \tilde{\mathbf{U}}_i^T \mathbf{n} \right\|^2 \right] \geq 1, \quad (36)$$

$$\sigma_i = 4 \text{tr} \left(\frac{1}{d_i} \mathbf{I} + \tilde{\mathbf{U}}_i^T \mathbf{R}_n \tilde{\mathbf{U}}_i \right) \quad (37)$$

$$\begin{aligned} &\leq 4(1 + \lambda_{\max}(\mathbf{R}_n) d_i) \\ &\leq 4(1 + \delta d_i), \end{aligned} \quad (38)$$

where the last inequality is due to the assumption that $\lambda_{\max}(\mathbf{R}_n) \leq \delta$.

For the second item in (35), it is also a sub-exponential random variable with expectation removed. Similar with (36) and (37), the calculation of its expectation μ_j and variance proxy

σ_j is as below.

$$\begin{aligned}
\mu_j &= \mathbb{E} \left[\|\mathbf{\Lambda}_{ji} \tilde{\mathbf{s}}\|^2 \right] + \mathbb{E} \left[\left\| \tilde{\mathbf{U}}_j^T \mathbf{n} \right\|^2 \right] \\
&= \frac{1}{d_i} \sum_{k=1}^{\min\{d_i, d_j\}} \cos^2 \theta_k^{i,j} + \text{tr} \left(\tilde{\mathbf{U}}_j^T \mathbf{R}_n \tilde{\mathbf{U}}_j \right) \\
&\leq \frac{1}{d_i} \text{aff}_{ji}^2 + \delta d_j, \\
\sigma_j &= 4 \text{tr} \left(\frac{1}{d_i} \mathbf{\Lambda}_{ji}^2 + \tilde{\mathbf{U}}_j^T \mathbf{R}_n \tilde{\mathbf{U}}_j \right) \\
&\leq 4 \left(\frac{1}{d_i} \text{aff}_{ji}^2 + \delta d_j \right).
\end{aligned}$$

Then the first item minus the second one is still a sub-exponential random variable, whose expectation is larger than

$$\mu_{ij} := 1 - \frac{1}{d_i} \text{aff}_{ji}^2 - \delta d_j. \quad (39)$$

The variance proxy is

$$\sigma_{ij} := 4 \left(1 + \frac{1}{d_i} \text{aff}_{ji}^2 + \delta(d_i + d_j) \right). \quad (40)$$

According to Bernsteins inequality, we have

$$P \left(\left\| \tilde{\mathbf{s}} + \tilde{\mathbf{U}}_i^T \mathbf{n} \right\|^2 - \left\| \mathbf{\Lambda}_{ij} \tilde{\mathbf{s}} + \tilde{\mathbf{U}}_j^T \mathbf{n} \right\|^2 < 0 \right) \leq \exp \left(-\frac{1}{2} \min \left\{ \frac{\mu_{ij}}{\sigma_{ij}}, \frac{\mu_{ij}^2}{\sigma_{ij}^2} \right\} \right). \quad (41)$$

Plugging (39) and (40) into (41), and then plugging (41) into (35), we can complete the proof.

F Covering Arguments

A convenient tool to discretize compact sets are nets. In our proof, we will only need to discretize the unit Euclidean sphere in the definition of ℓ_2 -norm. Let us recall a general definition of the ε -net.

Definition 6. (Vershynin, 2010) An ε -net in a totally bounded metric space (X, d) is a finite subset \mathcal{N} of X such that for any $x \in X$ we have

$$\min_{z \in \mathcal{N}} d(x, z) < \varepsilon.$$

The *metric entropy* of X is a function $N(X, \varepsilon)$ defined as the minimum cardinality of an ε -net of X .

The metric entropy of the Euclidean unit ball can be easily bounded as follows.

Lemma 10. (Foucart and Rauhut (2013), Proposition C.3) Let B_n be the unit ball in \mathbb{R}^n . Then

$$N(B_n, \varepsilon) \leq \left(1 + \frac{2}{\varepsilon}\right)^n.$$

ε -net allows us to evaluate the spectral norm of a square matrix \mathbf{A} by only investigating a discrete set.

Lemma 11. (Vershynin, 2010) Suppose \mathcal{N} is a $\frac{1}{4}$ -net of \mathbf{S}^{n-1} . Let \mathbf{A} be an $n \times n$ matrix. We have

$$\max_{\mathbf{x} \in \mathbf{S}^{n-1}} |\mathbf{x}^T \mathbf{A} \mathbf{x}| \leq 2 \max_{\mathbf{x} \in \mathcal{N}} |\mathbf{x}^T \mathbf{A} \mathbf{x}|.$$

References

- P.-A. Absil, R. Mahony, and R. Sepulchre. Riemannian geometry of grassmann manifolds with a view on algorithmic computation. *Acta Applicandae Mathematicae*, 80:199–220, 2004.
- P.-A. Absil, A. Edelman, and P. Koev. On the largest principal angle between random subspaces. *Linear Algebra and its Applications*, 414(1):288–294, 2006.
- R. I. Arriaga and S. Vempala. An algorithmic theory of learning: robust concepts and random projection. In *40th Annual Symposium on Foundations of Computer Science*, pages 616–623, 1999.
- R. Baraniuk, M. Davenport, R. Devore, and M. Wakin. A simple proof of the restricted isometry property for random matrices. *Constructive Approximation*, 28(28):253–263, 2015.
- A. Björck and G. H. Golub. Numerical methods for computing the angles between linear subspaces. *Mathematics of Computation*, 27:579–594, 1973.
- J. Candès, Emmanuel. The restricted isometry property and its implications for compressed sensing. *Comptes Rendus Mathématique*, 346(9–10):589–592, 2008.
- F. Deutsch. *The Angle Between Subspaces of a Hilbert Space*, volume 454. Springer, Dordrecht, 1995.
- S. Dirksen. Dimensionality reduction with subgaussian matrices: A unified theory. *Foundations of Computational Mathematics*, 16:1367–1396, 2016.

- D. L. Donoho. Compressed sensing. *IEEE Transactions on Information Theory*, 52(4):1289–1306, 2006.
- P. Drineas, M. W. Mahoney, and S. Muthukrishnan. Sampling algorithms for l_2 regression and applications. In *seventeenth annual ACM-SIAM symposium on Discrete algorithm*, 2006.
- A. Eftekhari and M. B. Wakin. What happens to a manifold under a bi-lipschitz map? *Discrete & Computational Geometry*, 57(3), 2017.
- A. Eftekhari, H. L. Yap, C. J. Rozell, and M. B. Wakin. The restricted isometry property for random block diagonal matrices. *Applied and Computational Harmonic Analysis*, 38:1–31, 2015.
- Y. C. Eldar and M. Mishali. Robust recovery of signals from a structured union of subspaces. *IEEE Transactions on Information Theory*, 55(11):5302–5316, 2009.
- E. Elhamifar and R. Vidal. Sparse subspace clustering. In *IEEE Conference on Computer Vision & Pattern Recognition*, 2009.
- E. Elhamifar and R. Vidal. Sparse subspace clustering: Algorithm, theory, and applications. *IEEE Transactions on Pattern Analysis and Machine Intelligence (PAMI)*, 35(11):2765–2781, 2013.
- S. Foucart and H. Rauhut. *A Mathematical Introduction to Compressive Sensing*. Springer Science & Business Media, 2013.
- P. Frankl and H. Maehara. Some geometric applications of the beta distribution. *Annals of the Institute of Statistical Mathematics*, 42(3):463–474, Sept. 1990.
- A. Galántai and C. J. Hegedűs. Jordan’s principal angles in complex vector spaces. *Numerical Linear Algebra with Applications*, 13:589–598, 2006.
- J. Hamm and D. D. Lee. Grassmann discriminant analysis: A unifying view on subspace-based learning. In *Proceedings of International Conference on Machine Learning (ICML)*, pages 376–383, July 2008.
- J. Haupt and R. Nowak. A generalized restricted isometry property. *University of Wisconsin Technical Report ECE-07-1*, 2007.
- R. Heckel and H. Bölcskei. Robust subspace clustering via thresholding. *IEEE Transactions on Information Theory*, 61(11):6320–6342, 2015.

- R. Heckel, M. Tschannen, and H. Bölcskei. Dimensionality-reduced subspace clustering. *Computer Science*, 2015.
- Y. Jiao, G. Li, and Y. Gu. Principal angles preserving property of gaussian random projection for subspaces. In *IEEE Global Conference on Signal and Information Processing (GlobalSIP)*, pages 318–322, 2017.
- Y. Jiao, Y. Chen, and Y. Gu. Subspace change-point detection: A new model and solution. *IEEE Journal of Selected Topics in Signal Processing*, 12(6):1224–1239, 2018a.
- Y. Jiao, X. Shen, and Y. Gu. Subspace principal angle preserving property of gaussian random projection. In *IEEE Data Science Workshop*, pages 115–119, June 2018b.
- W. B. Johnson and J. Lindenstrauss. Extensions of lipschitz maps into a hilbert space. *Israel Journal of Mathematics*, 26(189):189–206, 1984.
- C. Jordan. Essai sur la géométrie à n dimensions. *Bulletin de la Société mathématique de France*, 3:103–174, 1875.
- G. Li and Y. Gu. Restricted isometry property of gaussian random projection for finite set of subspaces. *IEEE Transactions on Signal Processing*, 66(7):1705–1720, 2018.
- G. Li, Q. Liu, and Y. Gu. Rigorous restricted isometry property of low-dimensional subspaces. *arXiv:1801.10058*, 2018.
- M. A. Lodhi and W. U. Bajwa. Detection theory for union of subspaces. *IEEE Transactions on Signal Processing*, 66(24):6347–6362, Dec 2018.
- D. Love and R. W. Heath. Limited feedback unitary precoding for orthogonal space-time block codes. *IEEE Transactions on Signal Processing*, 53:64–73, 2005a.
- D. J. Love and R. W. Heath. Limited feedback unitary precoding for spatial multiplexing systems. *IEEE Transactions on Information Theory*, 51:2967–2976, 2005b.
- X. Mao and Y. Gu. Compressed subspace clustering: A case study. In *2014 IEEE Global Conference on Signal and Information Processing (GlobalSIP)*, pages 453–457, 2014.
- B. McWilliams and G. Montana. Subspace clustering of high-dimensional data: a predictive approach. *Data Mining and Knowledge Discovery*, 28(3):736–772, 2014.
- L. Meng, G. Li, J. Yan, and Y. Gu. A general framework for understanding compressed subspace clustering algorithms. *IEEE Journal of Selected Topics in Signal Processing*, 12(6):1504–1519, 2018.

- J. Miao and A. Ben-Israel. On principal angles between subspaces in \mathbb{R}^n . *Linear Algebra and its Applications*, 171:81–98, 1992.
- J. Miao and A. Ben-Israel. Product cosines of angles between subspaces. *Linear Algebra and its Applications*, 237/238:71–81, 1996.
- S. Paul, C. Boutsidis, M. Magdon-Ismail, and P. Drineas. Random projections for support vector machines. In *Proceedings of the Sixteenth International Conference on Artificial Intelligence and Statistics*, pages 498–506, April 2013.
- X. Shen, Y. Jiao, and Y. Gu. Subspace data visualization with dissimilarity based on principal angle. In *IEEE Data Science Workshop*, pages 16–20, 2018.
- Q. Shi, C. Shen, R. Hill, and A. Hengel. Is margin preserved after random projection? In *Proceedings of International Conference on Machine Learning (ICML)*, 2012.
- M. Soltanolkotabi and E. J. Candes. A geometric analysis of subspace clustering with outliers. *The Annals of Statistics*, 40(4):2195–2238, 2012.
- R. Vershynin. Introduction to the non-asymptotic analysis of random matrices. *arxiv:1011.3027*, 2010.
- Y. Wang, Y. X. Wang, and A. Singh. A deterministic analysis of noisy sparse subspace clustering for dimensionality-reduced data. *IEEE Transactions on Information Theory*, 65(2):685–706, 2019.
- Y.-X. Wang and H. Yu. Noisy sparse subspace clustering. *Journal of Machine Learning Research (JMLR)*, pages 1–41, 2016.
- Y. C. Wong. Differential geometry of grassmann manifolds. *Proceedings of the National Academy of Sciences of the United States of America*, 57(3):589, 1967.
- X. Xu, G. Li, and Y. Gu. Johnson-lindenstrauss property implies subspace restricted isometry property. *arXiv:1905.09608*, 2019.
- K. Ye and L. Lim. Schubert varieties and distances between subspaces of different dimensions. *SIAM Journal on Matrix Analysis and Applications*, 37(3):1176–1197, 2016.
- C. You, D. P. Robinson, and R. Vidal. Scalable sparse subspace clustering by orthogonal matching pursuit. In *IEEE Conference on Computer Vision and Pattern Recognition (CVPR)*, pages 3918–3927, June 2016.
- Y. Yu, T. Wang, and R. J. Samworth. A useful variant of the davis–kahan theorem for statisticians. *Biometrika*, 102(2):315–323, 2014.

- H. Zhai, H. Zhang, L. Zhang, P. Li, and A. Plaza. A new sparse subspace clustering algorithm for hyperspectral remote sensing imagery. *IEEE Geoscience and Remote Sensing Letters*, 14(1):43–47, 2017.
- Y. Zhu, D. Huang, F. D. L. Torre, and S. Lucey. Complex non-rigid motion 3d reconstruction by union of subspaces. In *IEEE Conference on Computer Vision and Pattern Recognition (CVPR)*, pages 1542–1549, June 2014.